COUPLED OSCILLATORS NEAR RESONANCE

BY

LANCE ERIC ARSENAULT

B.S., Southeastern Massachusetts University, 1986
M.S., University of Illinois at Urbana-Champaign, 1989

THESIS

Submitted in partial fulfillment of the requirements
for the degree of Doctor of Philosophy in Physics
in the Graduate College of the
University of Illinois at Urbana-Champaign, 1996

Urbana, Illinois

COUPLED OSCILLATORS NEAR RESONANCE

Lance Eric Arsenault, Ph.D.
Department of Physics
University of Illinois at Urbana-Champaign, 1996
Alfred W. Hübler, Advisor

We study the dynamics of two conservative librating oscillators with perturbations from a linear displacement coupling and non-Hamiltonian forces such as damping. We examine the dynamics of these systems when they are near a resonance using secular perturbation theory. We show that near resonance a large class of driven oscillators and two coupled oscillators can be transformed to the same ordinary differential equations (ODEs). We consider two types of resonances: accidental and intrinsic. For an accidental resonance, we find that the dynamics near a resonance is a generalization of the standard Hamiltonian dynamics of two coupled conservative oscillators, which we call the standard equation. For an intrinsic resonance, we show that a primary resonance island can fill all of the available phase space. We derive expressions for the parameters in these ODEs. From a fixed-point analysis of these ODEs, we show that hard oscillators lock in-phase and soft oscillators lock out-of-phase. We develop a novel method for calculating accurate response curves for driven strongly nonlinear oscillators, where no existing method can give accurate results. We present a method for finding the steady state frequency of two coupled oscillators. We compare our theoretical predictions with computer simulations of many examples including: a sinusoidally driven highly nonlinear Duffing oscillator, and two coupled van der Pol oscillators with a highly nonlinear Duffing force.

To Rhonda and Holly

Acknowledgements

- Thank God I'm done.
- This work was supported in part by a grant from the Research Board of the University of Illinois.
- This material is based upon work supported by the National Science Foundation under Grant DMS-9105813.
- I thank the Beckman Institute of the University of Illinois for housing my office. Overall, it's a really nice place to work.
- Thanks to the Physics Department of the University of Illinois for helping finance my graduate education by providing me with teaching assistantships and research assistantships, without which I would not have done this. The teaching experience I have received is invaluable.
- Thanks to my advisor Dr. Alfred W. Hübler, whose jolly manner is a blessing to the world of science.
- I thank Dr. Atlee Jackson for stimulating discussions and fruitful suggestions.
- I thank Nick Weber, Ken Chang, and Mike Dueweke for being cool office mates.
- Special thanks to Dan Bensen and Gregor Dellemann, who actually used and critically analysed some of this work.
- Thanks to Prof. Paul Ukleja and Diane Cruz at the UMass (at Dartmouth) Physics Department.
- Thanks to Brian Rogers for helping me keep my sanity.
- Thanks to Laura Brandon for keeping me from becoming too sane, "heh heht huuht."
- Thanks to Shirley E. Ragusa.
- Finally, thanks to Rhonda for editing this and for being a supportive and loving wife.

Contents

List of Figures

Chapter 1

Introduction

1.1 Motivation

Weakly coupled nonlinear oscillators have been a popular research topic for many decades [1, 2, 3, 4, 5, 6, 7, 8]. There is a lot of phenomenological and numerical work done on these systems, for example by Bohr, et al [5]. There are many popular physical applications of such systems, including Josephson junctions [9], driven charge density waves [10], and oscillator models of Karman vortex streets in fluids [11].

There is a large body of literature concerned with linear oscillators that are perturbed by nonlinear forces [3, 12, 13]. In this literature, the nonlinearities in the systems studied are always added as a perturbation to a linear system. For example, Nayfeh and Mook [14] apply the method of multiple scales to a sinusoidally driven damped Duffing oscillator. The nonlinear force term is assumed to be small. For a first-order solution: A form of the solution (ansatz) to the ordinary differential equation (ODE) is posed that contains two different time scales, where one of the time scales is assumed to be slow compared to the other. With the introduction of these two time scales, they assume that the amplitude and the phase difference between the driver and driven oscillator are both dependent on the slow time variable, and the phase of the oscillator is dependent on the faster time variable. The ansatz is a sinusoid with the two time scales included. This ansatz is plugged into the ODE and any unknown constants are solved for by setting any secular terms to zero. With the constants solved, the ansatz is now the steady state solution to the ODE. This method is based on the assumption that the nonlinear forcing terms are small. So this method usually will not give accurate results when it is applied to highly nonlinear oscillators.

Chirikov [15] shows how the dynamics of a large class of two weakly coupled conservative oscillators near a resonance can be approximated by the dynamics of a pendulum. In this theory, called secular perturbation theory [1, 2], canonical action-angle variables are introduced, secular terms in the equations of motion are removed with a special change of variables, the Hamiltonian is averaged over one of the fast angle variables, and the Hamiltonian is expanded about the resonance. This reduces the original four ODE two-oscillator system to a two ODE dynamical system. This averaging is responsible for removing the stochastic dynamics between the Kol'mogorov-Arnol'd-Moser (KAM) [16] surfaces. This method can be applied to highly nonlinear systems. But this analysis can only be applied to Hamiltonian systems, so non-Hamiltonian forces like damping cannot be added to the system.

We study the same systems as Chirikov with the addition of non-Hamiltonian perturbations, such as damping and anti-damping. We show that for two identical oscillators the dynamics of this system near a resonance can be approximated by the dynamics of a damped pendulum. If the oscillators are not identical, there are more terms in the equations of motion than a damped pendulum.

Because of the non-Hamiltonian forces such as damping, our method differs from Chirikov in that we average and expand the equations of motion. As opposed to using generating functions of Hamiltonian mechanics, we introduce action-angle variables by using transformation functions to define them. Thus, when we transform to action-angle variables we are not restricted to having just Hamiltonian perturbations.

With the addition of dissipative forces, phase-space area will not be conserved as it is in Hamiltonian systems. Of special interest is the phase-space contraction due to damping forces when the two oscillators are near a resonance. This can cause the system to evolve into a state we call phase-locked, which is where the ratio of the phases of the two oscillators is a rational number. By extending this method of secular perturbation theory, we can study the important phenomenon of phase-locking, which is not present in Hamiltonian systems.

In contrast to the work of Nayfeh and Mook, we study oscillators that may have large nonlinear forces that are not treated as perturbations. Nayfeh and Mook's methods can be applied to dissipative systems, but they are restricted to systems where the nonlinear forces are treated as perturbations. These methods usually will not give accurate results when applied to systems with highly nonlinear oscillators.

1.2 Scope

In this discourse, we study the dynamics of two conservative librating oscillators with perturbations from a linear displacement coupling and non-Hamiltonian forces such as damping.

We refer to a periodically driven oscillator as a system of two coupled oscillators where the coupling to the driver oscillator is turned off. So we say that there is a one-way coupling. With this idea, we can study both a driven oscillator and two coupled oscillators with the same model. For all cases in our study, we start with a model of this system as four first-order ODEs and in all cases reduce these systems to lower-dimensional ODE systems.

We examine the dynamics of these systems when they are near a resonance. We define resonance to be the state of a system when the ratio of the frequencies of the two unperturbed oscillators is a rational number. In all cases studied, we assume that we are near a resonance.

In chapter 2 we study the case when the resonance is due to a chance coincidence of the values of the two frequencies as the actions of the two oscillators are varied. We call this kind of resonance an accidental resonance. We find that the dynamics near an accidental resonance can be represented in a standard form with two first-order ODEs that we call the standard equation [17]. Next we do a linear fixed-point analysis of the standard equation. We define phase-locked to be the state of our system when the ratio of the angle of the two oscillators is a rational number. A primary resonance is a resonance when the frequencies of the two oscillators are equal. We define a hard (soft) oscillator to be an oscillator that has a frequency that will increase (decrease) when the action in the oscillator is increased. From the standard equation, we find for a primary resonance that when two hard oscillators phase-lock they will always phase-lock in phase and when two soft oscillators phase-lock they will always phase-lock out of phase. Also we find that for two identical oscillators the standard equation takes the form of a damped pendulum.

In chapter 3 we study the case when the resonance condition is always satisfied for all initial conditions. We call this type of resonance an intrinsic resonance. We restrict this study to the primary resonance; no damping is present and the total energy in conserved. We find this case interesting because for some initial conditions the two oscillators will exchange all of the energy in the system back and forth indefinitely. We conclude the chapter by demonstrating this with an example, by coupling a soft and a hard Duffing oscillator.

In chapter 4 we develop a novel method for calculating response curves for periodically driven oscillators. We illustrate the use of this new method on a classic example, a sinusoidally driven damped Duffing oscillator.

In chapter 5 we apply the new techniques from chapters 2 and 4 to a sinusoidally driven highly nonlinear Duffing oscillator. We make the Duffing oscillator highly nonlinear by making the cubic force term much larger than the linear force term. We consider the linear force term to be a perturbation in the system. We calculate the corresponding standard equation for this system. We compare numerical simulations of the exact system with that of the standard equation. We compare the calculated response curves with numerical simulations of the exact system.

In chapter 6 we study two-way coupled oscillators and their steady state dynamics at phase-locking. First we define what we call locking frequency. Then we proceed to find an expression for this locking frequency in terms of the parameters in the original equations of motion. In the process, we show how some of the assumptions made in deriving the standard equation, of chapter 2, can be satisfied.

In chapter 7 we apply the new techniques from chapters 2 and 6 to two coupled (two-way coupling) van der Pol oscillators with a highly nonlinear Duffing force. We calculate the corresponding standard equation for this system. We compare numerical simulations of the exact system with that of the standard equation. We compare the calculated locking frequency with numerical simulations of the exact system.

In chapter 8 we discuss this work in retrospect and prospective future work.

In appendix A we define the transformation functions that are used in every chapter of this text. These transformation functions are used to define what we call generalized action-angle variables. These variables are a generalization of the usual action-angle variables in the sense that they can be used in dissipative systems where the usual action-angle variables cannot.

In appendix B we study the averaging method that is used throughout this discourse. We show what averaged equations represent and how well they are represented.

Chapter 2

Small Resonances: The Standard Equation

The following is a generalization of the study presented by Arsenault and Hübler [17] in which they studied primary resonances, which is when two oscillators have the same frequency. Here we will study a general resonance, which is when the ratio of the two oscillator frequencies is a rational number.

In this chapter we derive a standard equation of motion for a general class of two coupled librating oscillators that are near an accidental resonance, then we do a linear fixed-point analysis of the standard equation, and finally we discuss some interesting predictions from the standard equation.

2.1 Derivation of the Standard Equation

We investigate the system of two coupled oscillators of the form

$$\dot{x}_i = \frac{p_i}{m_i}, \tag{2.1}$$

$$\dot{p}_i = F_i(x_i) + \epsilon\Gamma_i(x_i, p_i) + \epsilon k_i x_j, \tag{2.2}$$

$$F_i(x_i) \equiv -\frac{dU_i(x_i)}{dx_i}, \tag{2.3}$$

where $i, j = 1, 2$, $i \neq j$, x_i is a displacement, k_i and m_i are constants, ϵ is a small constant number, and U_i is the potential of the i-th oscillator. We restrict our analysis to solutions of Eqs. (2.1) and (2.2) that are bounded in some finite region of x_1, x_2, p_1, and p_2 space for all t. [1] In this section, we look at both the case of a driven oscillator (one-way coupling) and the case of two coupled oscillators with two-way coupling. For the case of a driven oscillator, we set $k_1 \equiv 0$, $k_2 \equiv k$, and $\Gamma_1 \equiv 0$. For the case with two-way coupling, we set $k_1 \equiv k$ and $k_2 \equiv k$.

Next, we change variables x_i and p_i to their corresponding action-angle variables, J_i and ϕ_i, by using their corresponding transformation functions, $X_i(J_i, \phi_i)$, $P_i(J_i, \phi_i)$, $K_i(J_i)$, and $\omega_i(J_i)$ where $i = 1, 2$, as explained in appendix A.

In what follows, we investigate the dynamics of Eqs. (2.1) and (2.2) close to a general resonance. So we define the resonance condition by

$$\frac{\omega_1(J_1)}{\omega_2(J_2)} = \frac{r}{s}, \tag{2.4}$$

where r and s are integers. In what follows we will assume that at least one of the oscillators has an action dependent angular frequency. Because of this, Eq. (2.4) can be satisfied by dynamically changing the values of the action of the oscillators. Such is not the case for the resonance of two coupled linear oscillators, where the resonance condition can only be satisfied by a parametric variation. We will assume that the resonance condition is satisfied only for particular values of J_1 and J_2 (accidental resonance) and not for all values of J_1 and J_2.

In order to avoid secular terms, we transform our equations to a rotating frame by using the following change of dynamical variables

$$\Phi \equiv r\phi_2 - s\phi_1, \tag{2.5}$$

$$\Omega \equiv r\omega_2(J_2) - s\omega_1(J_1), \tag{2.6}$$

$$I \equiv \begin{cases} rJ_1 & \text{if case: driven} \\ sJ_2 + rJ_1 & \text{if case: two-way coupling} \end{cases}, \tag{2.7}$$

[1] We are excluding the case of rotating oscillators.

$$\phi \equiv \frac{\phi_1}{r}. \tag{2.8}$$

The choice of the variables Ω and ϕ is somewhat arbitrary. The results are the same if ϕ is defined as any linear combination of ϕ_1 and ϕ_2 that is linearly independent of Φ. For the results we are seeking Ω can be any nontrivial function of J_1 and J_2 that is functionally independent of I. For convenience we have chosen Ω so that $\Omega = 0$ is equivalent to the resonance condition, Eq. (2.4).

From Eqs. (A.22), (A.40), and (A.41) of appendix A and Eqs. (2.1)–(2.8), the equations of motion of Φ, Ω, I, and ϕ may be written as

$$\dot{\Phi} = \Omega - \epsilon r \frac{\partial X_2}{\partial J_2} \left(\Gamma_2 + k_2 X_1\right) + \epsilon s \frac{\partial X_1}{\partial J_1} \left(\Gamma_1 + k_1 X_2\right), \tag{2.9}$$

$$\dot{\Omega} = \frac{\epsilon r}{m_2 \omega_2} \frac{d\omega_2}{dJ_2} P_2 \left(\Gamma_2 + k_2 X_1\right) - \frac{\epsilon s}{m_1 \omega_1} \frac{d\omega_1}{dJ_1} P_1 \left(\Gamma_1 + k_1 X_2\right), \tag{2.10}$$

$$\dot{I} = \frac{\epsilon}{m_2 \omega_2} \frac{\partial I}{\partial J_2} P_2 \left(\Gamma_2 + k_2 X_1\right) + \frac{\epsilon}{m_1 \omega_1} \frac{\partial I}{\partial J_1} P_1 \left(\Gamma_1 + k_1 X_2\right), \tag{2.11}$$

$$\dot{\phi} = \frac{\omega_1}{r} - \frac{\epsilon}{r} \frac{\partial X_1}{\partial J_1} \left(\Gamma_1 + k_1 X_2\right), \tag{2.12}$$

where it is assumed that all quantities on the right side of the equations can be written as functions of just Φ, Ω, I, and ϕ. Eqs. (2.9)–(2.12) are exact.

The two-oscillator system is near the resonance of Eq. (2.4), so we impose that Ω is of size of order $\epsilon^{\frac{1}{2}}$. By Eqs. (2.9)–(2.12), Φ, Ω, and I are changing, by at least a factor of order $\epsilon^{\frac{1}{2}}$, more slowly than ϕ. Because of this, we approximate the dynamics of Φ, Ω, and I with the dynamics of a ϕ-averaged version of these equations of motion by averaging over the fast variable ϕ. References [1, 2, 7, 18, 19] illustrate an averaging method similar to this. In appendix B we show to what order the ϕ-averaged equations of motion are the same as time averaged equations of motion, where the time averaging is over the time it takes ϕ to change by 2π.

We define a ϕ-averaged function $\langle \xi \rangle_\phi(\Phi, \Omega, I)$ by

$$\langle \xi \rangle_\phi(\Phi, \Omega, I) \equiv \frac{1}{2\pi} \int_0^{2\pi} \xi(\Phi, \Omega, I, \phi)\, d\phi\,. \tag{2.13}$$

In what follows, we use

$$X_i(J_i, \phi_i) = \sum_{l=0}^{\infty} C_{i,l}(J_i) \cos(l\phi_i), \tag{2.14}$$

$$P_i(J_i, \phi_i) = -m_i\omega_i(J_i)\sum_{l=1}^{\infty} lC_{i,l}(J_i)\sin(l\phi_i), \tag{2.15}$$

where $i = 1, 2$.

Next we approximate the right-hand side of Eqs. (2.9)–(2.12) by the corresponding ϕ-averaged values. We consider the case where the Fourier coefficients $C_{i,l}(J_i)$, as defined in Eqs. (2.14) and (2.15), decrease rapidly with increasing l. So after averaging we will keep the non-zero Φ-dependent terms with the lowest Fourier harmonics and throw away all Φ-dependent terms with higher Fourier harmonics. These two approximations, averaging and then dropping harmonics, give

$$\begin{aligned}
\dot{\Phi} &= \Omega - \epsilon r\left\langle \frac{\partial X_2}{\partial J_2}\Gamma_2\right\rangle_\phi + \epsilon s\left\langle \frac{\partial X_1}{\partial J_1}\Gamma_1\right\rangle_\phi - \epsilon r k_2\frac{dC_{2,0}}{dJ_2}C_{1,0} + \epsilon s k_1\frac{dC_{1,0}}{dJ_1}C_{2,0} \\
&\quad -\frac{\epsilon}{2}\left(rk_2\frac{dC_{2,r}}{dJ_2}C_{1,s} - sk_1\frac{dC_{1,s}}{dJ_1}C_{2,r}\right)\cos\Phi, && (2.16)\\
\dot{\Omega} &= \frac{\epsilon r}{m_2\omega_2}\frac{d\omega_2}{dJ_2}\langle P_2\Gamma_2\rangle_\phi - \frac{\epsilon s}{m_1\omega_1}\frac{d\omega_1}{dJ_1}\langle P_1\Gamma_1\rangle_\phi \\
&\quad -\frac{\epsilon}{2}C_{1,s}C_{2,r}\left(r^2k_2\frac{d\omega_2}{dJ_2} + s^2k_1\frac{d\omega_1}{dJ_1}\right)\sin\Phi, && (2.17)\\
\dot{I} &= \frac{\epsilon}{m_2\omega_2}\frac{\partial I}{\partial J_2}\langle P_2\Gamma_2\rangle_\phi + \frac{\epsilon}{m_1\omega_1}\frac{\partial I}{\partial J_1}\langle P_1\Gamma_1\rangle_\phi, && (2.18)\\
\dot{\phi} &= \frac{\omega_1}{r} - \frac{\epsilon}{r}\left\langle \frac{\partial X_1}{\partial J_1}\Gamma_1\right\rangle_\phi - \epsilon\frac{k_1}{r}\frac{dC_{1,0}}{dJ_1}C_{2,0} - \frac{\epsilon k_1}{2r}\frac{dC_{1,s}}{dJ_1}C_{2,r}\cos\Phi, && (2.19)
\end{aligned}$$

where all the terms with $\langle\ \rangle_\phi$ do not depend on Φ.

Eq. (2.19) is not of interest at present but will be used in chapter 6 to find an approximate expression for the angular frequency of the oscillators when they phase-lock.

We expand the right sides of Eqs. (2.16)–(2.18) in a Taylor series about $\Omega = 0$ and about $I = I_0$, where I_0 is a constant. The value of I_0 we get from the condition $\dot{I}(\Omega = 0, I = I_0) = 0$, where $\dot{I}$ is approximated by Eq. (2.18). The expanded equations of motion are approximations of the dynamics of the system in a small volume of the Φ, Ω, and I phase space, which is the shape of a box of sides of size of order 1 by $\epsilon^{\frac{1}{2}}$ by ϵ respectively.

Φ is of size of order 1. $\dot{\Phi}$ is expanded to first order in ϵ. We wish to study this system near resonance so we impose that Ω is of size of order $\epsilon^{\frac{1}{2}}$. To be consistent with the expansion of $\dot{\Phi}$, $\dot{\Omega}$ is expanded to order $\epsilon^{\frac{3}{2}}$. $I - I_0$ is of size of order ϵ. Therefore, the lowest order term that depends on I in the expansion of $\dot{\Phi}$ and $\dot{\Omega}$ is of size of order ϵ^2. So by expanding to the above stated orders in ϵ, the $\dot{\Phi}$ and the $\dot{\Omega}$ equations do not depend on I. The above restrictions and approximations enable us to study a two-dimensional system in the variables Φ and Ω, which evolve independently of I and ϕ.

Expanding Eqs. (2.16) and (2.17) gives

$$\dot{\Phi} = \Omega + a_1 + a_2 \cos\Phi, \tag{2.20}$$

$$\dot{\Omega} = a_3 + a_4 \sin\Phi + a_5\Omega + a_6\Omega\sin\Phi, \tag{2.21}$$

where a_i $(i = 1, 2, 3, 4, 5, 6)$ are constants of size of order ϵ.

We call Eqs. (2.20) and (2.21) the standard equation because it describes the dynamics about resonance for a more general class of two coupled oscillators than Lichtenberg and Lieberman's standard Hamiltonian [1].

To derive expressions for the a_i coefficients in the standard equation we use the result

$$\frac{\partial}{\partial\Omega} = \frac{1}{r^2\frac{d\omega_2}{dJ_2} + s^2\frac{d\omega_1}{dJ_1}}\left(r\frac{\partial}{\partial J_2} - s\frac{\partial}{\partial J_1}\right), \tag{2.22}$$

which comes from the definitions of Ω and I in the two-way coupling case. We can express the a_i coefficients as:

$$a_1 = -\epsilon r\left\langle\frac{\partial X_2}{\partial J_2}\Gamma_2\right\rangle_\phi + \epsilon s\left\langle\frac{\partial X_1}{\partial J_1}\Gamma_1\right\rangle_\phi - \epsilon r k_2\frac{dC_{2,0}}{dJ_2}C_{1,0} + \epsilon s k_1\frac{dC_{1,0}}{dJ_1}C_{2,0}\Bigg|_{\Omega=0,I=I_0}, \tag{2.23}$$

$$a_2 = -\frac{\epsilon}{2}\left(rk_2\frac{dC_{2,r}}{dJ_2}C_{1,s} - sk_1\frac{dC_{1,s}}{dJ_1}C_{2,r}\right)\Bigg|_{\Omega=0,I=I_0}, \tag{2.24}$$

$$a_3 = \frac{\epsilon r}{m_2\omega_2}\frac{d\omega_2}{dJ_2}\langle P_2\Gamma_2\rangle_\phi - \frac{\epsilon s}{m_1\omega_1}\frac{d\omega_1}{dJ_1}\langle P_1\Gamma_1\rangle_\phi\Bigg|_{\Omega=0,I=I_0}, \tag{2.25}$$

$$a_4 = -\frac{\epsilon}{2}C_{1,s}C_{2,r}\left(r^2k_2\frac{d\omega_2}{dJ_2} + s^2k_1\frac{d\omega_1}{dJ_1}\right)\Bigg|_{\Omega=0,I=I_0}, \tag{2.26}$$

$$a_5 = \frac{\epsilon}{r^2\frac{d\omega_2}{dJ_2} + s^2\frac{d\omega_1}{dJ_1}}\left[\frac{r^2}{m_2}\frac{\partial}{\partial J_2}\left(\frac{1}{\omega_2}\frac{d\omega_2}{dJ_2}\langle P_2\Gamma_2\rangle_\phi\right) + \frac{s^2}{m_1}\frac{\partial}{\partial J_1}\left(\frac{1}{\omega_1}\frac{d\omega_1}{dJ_1}\langle P_1\Gamma_1\rangle_\phi\right)\right]\Bigg|_{\Omega=0,I=I_0} \tag{2.27}$$

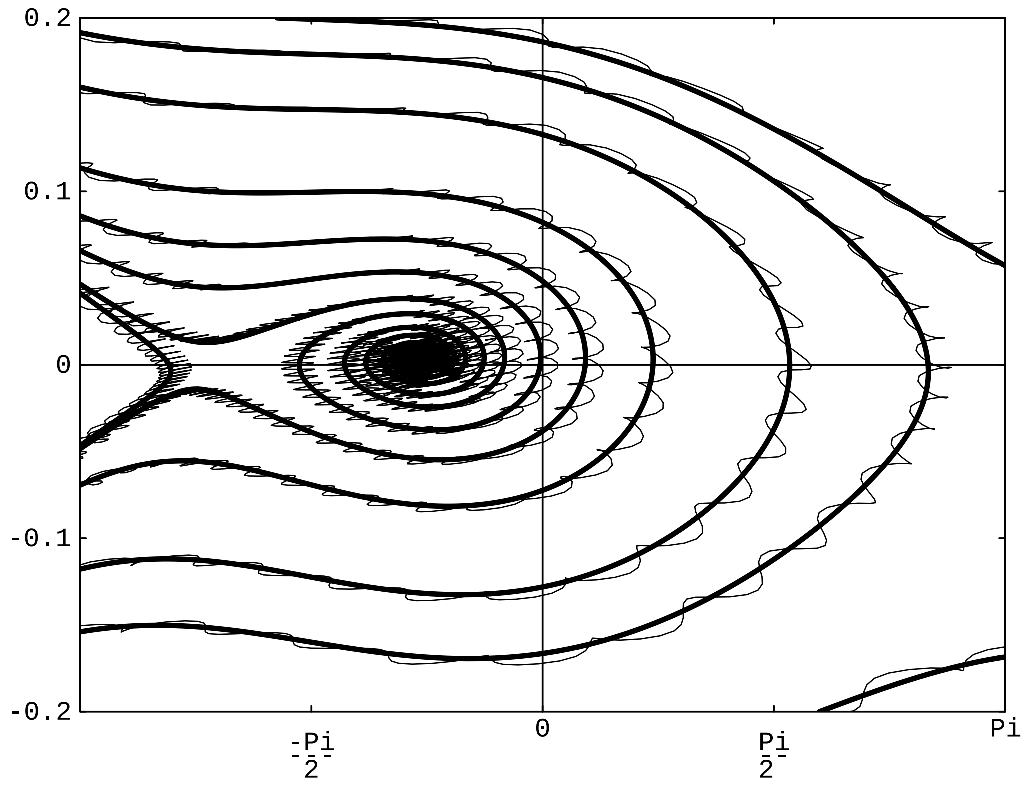

Figure 2.1: Ω vs. Φ phase plot of the driven oscillator Eqs. (2.1)–(2.3) with $F_1(x_1) = -\omega_1^2 x_1$, $F_2(x_2) = -x^3$, $\epsilon\Gamma_2(x_2, p_2) = -\gamma p_2$, and with parameters: the amplitude of the driver $A_1 = 0.01$, $\omega_1 = 0.8$, and $\gamma = 0.01$. Standard equation [thick lines]. Exact equations of motion [thin wiggly lines]. See details about this system in chapter 5.

$$a_6 = \frac{\epsilon}{r^2 \frac{d\omega_2}{dJ_2} + s^2 \frac{d\omega_1}{dJ_1}} \left(r \frac{\partial}{\partial J_2} - s \frac{\partial}{\partial J_1} \right) \left[-\frac{1}{2} C_{1,s} C_{2,r} \left(r^2 k_2 \frac{d\omega_2}{dJ_2} + s^2 k_1 \frac{d\omega_1}{dJ_1} \right) \right] \Bigg|_{\Omega=0, I=I_0} \tag{2.28}$$

where the last step is to evaluate the expressions at $\Omega = 0$ and $I = I_0$. These coefficients are the same for both the driven and the two-way coupling cases.[2]

Fig. 2.1 shows a Ω vs. Φ phase plot of the standard equation, Eqs. (2.20)–(2.21), compared with that from the exact equations of motion, for a driven oscillator.

[2]Recall that for the driven case, $k_1 = 0$ and $\Gamma_1 = 0$, and the condition $I = I_0$ is not necessary because $\dot{I} = 0$.

2.2 Linear Fixed-Point Analysis of the Standard Equation

An analytic expression for the fixed points of Eqs. (2.20) and (2.21) cannot, in general, be found. We can, however, find analytic expressions for the fixed points to first order in ϵ. The right side of Eqs. (2.21) and (2.20) is periodic in Φ with a period of 2π. Therefore, the Φ–Ω phase-space portrait will be spatially periodic in Φ with a period of 2π.

To first order, if $|a_4| > |a_3|$, there are two fixed points in Eqs. (2.20) and (2.21) in the interval $0 \leq \Phi < 2\pi$: one at

$$\Phi_{f,1} = \arcsin\left(\frac{a_3}{a_4}\right) + \pi \mod 2\pi, \tag{2.29}$$

$$\Omega_{f,1} = -a_1 + a_2\sqrt{1 - \left(\frac{a_3}{a_4}\right)^2}, \tag{2.30}$$

and one at

$$\Phi_{f,2} = -\arcsin\left(\frac{a_3}{a_4}\right) \mod 2\pi, \tag{2.31}$$

$$\Omega_{f,2} = -a_1 - a_2\sqrt{1 - \left(\frac{a_3}{a_4}\right)^2}, \tag{2.32}$$

where $\Phi_{f,i}$, $i = 1, 2$, is a fixed-point value of Φ, and $\Omega_{f,i}$, $i = 1, 2$, is a fixed-point value of Ω.

To lowest order in ϵ, the characteristic exponents ($\Phi - \Phi_{f,i}, \Omega - \Omega_{f,i} \sim e^{\lambda_i t}$) are given by

$$\lambda_i = \frac{1}{2}\left(\frac{a_3 a_2}{a_4} + a_5 - \frac{a_3 a_6}{a_4}\right) \pm \sqrt{-\frac{a_4}{a_2}\left(\Omega_{f,i} + a_1\right)}, \tag{2.33}$$

where $i = 1, 2$ and the $\pm$ gives two values of λ_i for each i.

If $|a_4| < |a_3|$ then, to first order in ϵ, there are no fixed points in the standard equation. This corresponds to a passive resonance, which is when the two oscillators will not phase-lock near the resonance.

If $|a_4| > |a_3|$, one of the fixed points is a saddle point and the other is a focal point. The focal point is the fixed point with the characteristic exponents, λ_1 or λ_2, that has an imaginary part. Eqs. (2.30), (2.32), and (2.33) show that this depends on just the sign of the a_4 coefficient, Eq. (2.26), that in turn depends on the sign of the Fourier coefficients and the derivatives of the angular frequency with respect to action, both evaluated at the resonant expansion point. The focal point is of special interest to us because it corresponds to the point where the two oscillators can phase-lock. When two oscillators phase-lock, the motion of both oscillators is periodic. The saddle point also corresponds to a solution when the motion of both oscillators is periodic, but this solution is always unstable. The Φ–Ω phase plot in Fig. 2.1 shows these two fixed points.

There are bifurcation lines at $|a_3| = |a_4|$ where the saddle point and the focus collide and become one fixed point.

2.3 Deductions from the Standard Equation

2.3.1 Hard Oscillators Lock In-Phase, Soft Oscillators Lock Out-of-Phase

Here we consider a primary resonance ($r = s = 1$). For a primary resonance the idea of oscillators being in-phase and out-of-phase is clear, but that is not the case for a general resonance. Phase locking occurs at a focal point in Φ–Ω space. A linear fixed-point analysis (section 2.2) of the standard equation, Eqs. (2.20) and (2.21), with $|a_4| \gg |a_3|$ gives us the result that there is a focal point at the fixed point with $\Phi_{f,1} \approx \pi$ if $a_4 > 0$, and at the point with $\Phi_{f,2} \approx 0$ if $a_4 < 0$.

$$a_4 = -\frac{\epsilon}{2} C_{1,1} C_{2,1} \left(k_1 \frac{d\omega_1}{dJ_1} + k_2 \frac{d\omega_2}{dJ_2} \right) \bigg|_{\Omega=0, I=I_0}, \tag{2.34}$$

where all quantities are evaluated at $\Omega = 0$ and $I = I_0$.

We define the nonlinearity parameter by

$$G \equiv \frac{1}{k_2} \left(k_1 \frac{d\omega_1}{dJ_1} + k_2 \frac{d\omega_2}{dJ_2} \right) \bigg|_{\Omega=0, I=I_0}, \tag{2.35}$$

where all quantities are evaluated at $\Omega = 0$ and $I = I_0$. For the case of one-way coupling, G is the action-frequency coupling of the driven oscillator, $\frac{d\omega_2}{dJ_2}$. For the case of two-way coupling, G is the sum of the action-frequency coupling of the two oscillators, $\frac{d\omega_1}{dJ_1} + \frac{d\omega_2}{dJ_2}$.

By construction, $C_{1,1}$ and $C_{2,1}$ are both positive. If the sign of G is negative then the focal point is at $\Phi_{f,1} \approx \pi$, and if G is positive then the focal point is at $\Phi_{f,2} \approx 0$. We define an oscillator with a frequency that decreases with increasing action ($\frac{d\omega}{dJ} < 0$) to be a soft oscillator, and an oscillator with a frequency that increases with increasing action ($\frac{d\omega}{dJ} > 0$) to be a hard oscillator. This shows that if the coupling forces are larger than other perturbations (i.e., $|a_4| \gg |a_3|$) and if the coupled oscillator system can phase-lock (i.e., $\mathrm{Re}[\lambda_i] < 0$) then if $G > 0$ (hard oscillators) the oscillators phase-lock in-phase ($\Phi \to 0$), and if $G < 0$ (soft oscillators) the oscillators phase-lock out-of-phase ($\Phi \to \pi$). Thus, we get the result that two coupled hard oscillators will phase-lock in-phase and two coupled soft oscillators will phase-lock out-of-phase.

This result can be understood by a more intuitive argument. By inspection of Eq. (2.6) and Eq. (2.17), the change in the action of the i-th oscillator, due to just coupling, on average over one cycle, is given by

$$\dot{J}_i \approx -\frac{\epsilon}{2} k C_{1,1} C_{2,1} sin(\phi_i - \phi_j), \tag{2.36}$$

where $i, j = 1, 2$ and $i \neq j$. This shows that on average over one cycle the oscillator with the lagging angle will have its action increased while the action of the oscillator with the leading angle will have its action decreased by the same amount. This is true to first order in ϵ and assuming that coupling terms are much larger than all other perturbations. The "other perturbations" (i.e., damping terms) are necessary to cause the phase-space contraction (i.e., phase-locking) but don't affect the dynamics to first order in ϵ by assertion.

With this result, Eq. (2.36), we see that an angle difference of 0 and π will cause the actions of both oscillators not to change. In other words, in-phase and out-of-phase are equilibrium states of the two coupled oscillators. For two hard oscillators the lagging oscillator will gain action while the leading oscillator loses action, which will cause the lagging oscillator's frequency to increase and the leading oscillator's frequency to decrease, which will, in turn, cause the angle (phase) difference to decrease until the lagging oscillator and the leading oscillator switch relative phases. So we see that the

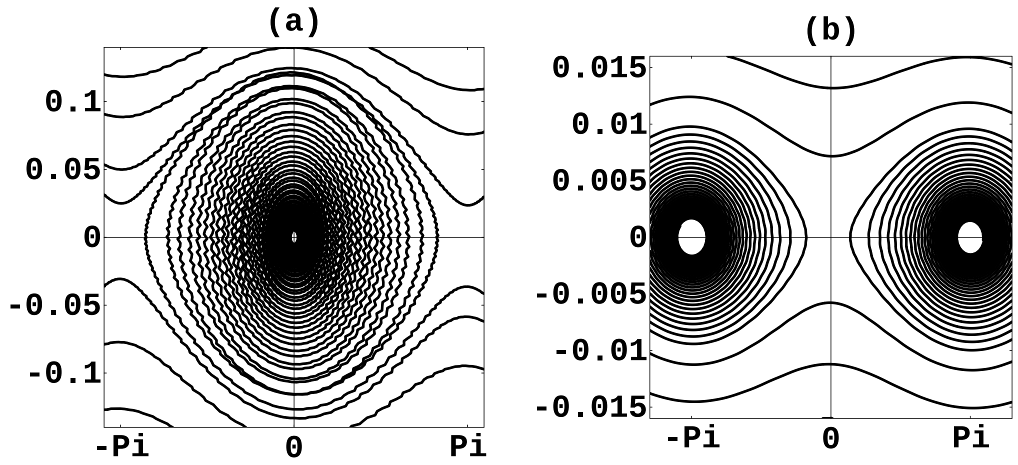

Figure 2.2: Ω vs. Φ phase plot from a numerical simulation of the two coupled identical oscillators: $\ddot{x}_i = -x_i - \beta x_i^3 + \eta(1 - x_i^2)\dot{x}_i + kx_j$, $i, j = 1, 2$, and $i \neq j$. (a) Two identical hard oscillators with $\beta = 0.1$, $\eta = 2 \times 10^{-3}$, and $k = 1 \times 10^{-2}$. (b) Two identical soft oscillators: $\beta = -0.01$, $\eta = 1 \times 10^{-4}$, and $k = 9 \times 10^{-4}$.

in-phase equilibrium state is a stable state for two hard oscillators. Similar reasoning shows that the out-of-phase equilibrium state is a stable state for two soft oscillators. This same reasoning shows that the out-of-phase equilibrium state is an unstable state for two hard oscillators and that the in-phase equilibrium state is an unstable state for two soft oscillators.

Fig. 2.2a (2.2b) is a Φ–Ω phase plot from a simulation of two coupled hard (soft) oscillators. It shows how the hard oscillators phase-lock in-phase and the soft oscillators phase-lock out-of-phase.

2.3.2 Two Coupled Identical Oscillators

Here again we consider a primary resonance ($r = s = 1$). We define two identical oscillators to be two oscillators that have the same equations of motion when $k_i = 0$ for $i = 1, 2$. Inspection of the a_i ($i = 1, 2, 3, 4, 5, 6$) coefficients of the standard equation, Eqs. (2.23)–(2.28), shows that for two identical oscillators a_1, a_2, a_3, and a_6 are zero.

With this, the standard equation is given by

$$\dot{\Phi} = \Omega, \tag{2.37}$$

$$\dot{\Omega} = a_4 \sin\Phi + a_5\Omega, \tag{2.38}$$

where

$$a_4 = \left[-\epsilon k C_{1,1}^2 \frac{d\omega_1}{dJ_1}\right]\Bigg|_{\Omega=0, I=I_0}, \tag{2.39}$$

$$a_5 = \left[\frac{\epsilon}{m_1 \frac{d\omega_1}{dJ_1}} \frac{\partial}{\partial J_1}\left(\frac{1}{\omega_1}\frac{d\omega_1}{dJ_1}\langle P_1\Gamma_1\rangle_\phi\right)\right]\Bigg|_{\Omega=0, I=I_0}, \tag{2.40}$$

where the expressions for a_4 and a_5 are evaluated at $\Omega = 0$ and $I = I_0$. We see that the dynamics of two coupled identical oscillators with two-way coupling, near resonance, is that of a damped pendulum. So if $a_5 < 0$, the two oscillators phase-lock for all initial conditions in the Φ–Ω plane that are near the primary resonance, except for initial conditions on a line that is part of the separatrix that flows into the saddle point in the Φ–Ω phase-space, which has a measure of zero.[3]

Fig. 2.2 is a Φ–Ω phase plot from a simulation of two coupled identical oscillators. Notice how the phase plots look like that of a damped pendulum.

[3]This exception is like balancing a pendulum in the unstable inverted position.

Chapter 3

Super Resonances

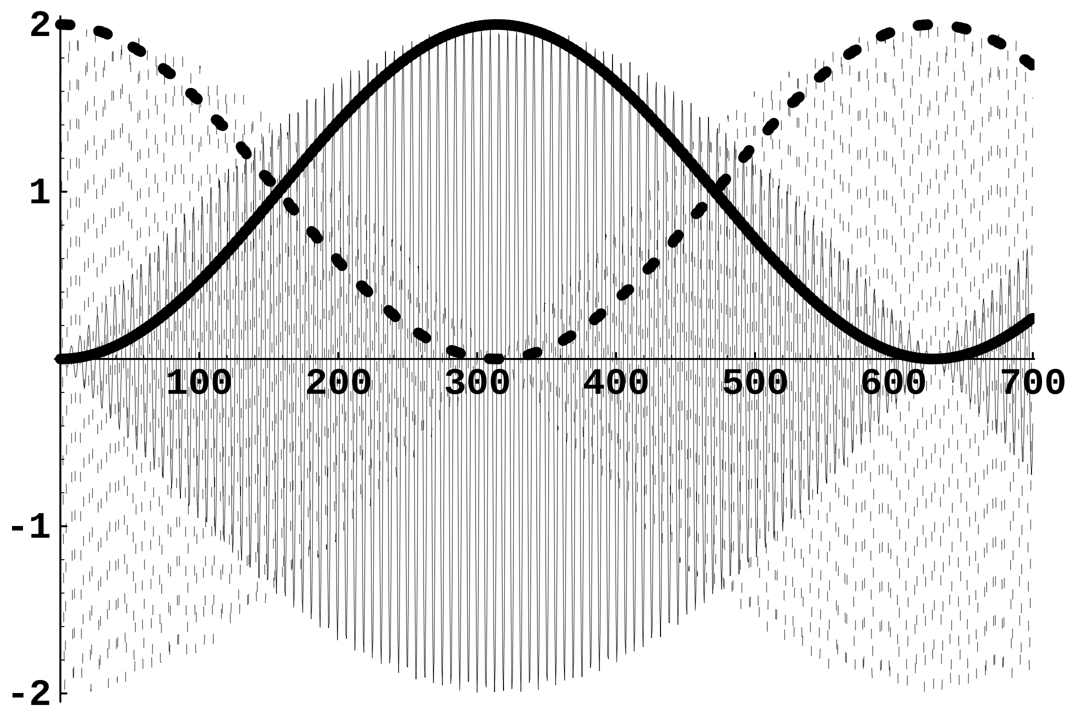

Figure 3.1: Plots of energies (H_1, H_2) and positions (x_1, x_2) vs. time (t) for the two coupled linear oscillators in Eqs.(3.1) and (3.2) with the papameters $k = 0.01$ and $\omega_1 = \omega_2 = 1$ and with the initial conditions $x_1(0) = 2$, $\dot{x}_1(0) = 0$, $x_2(0) = 0$, and $\dot{x}_2(0) = 0$. Energy of oscillator one: $H_1 \equiv \frac{1}{2}\omega_1^2 x_1^2 + \frac{1}{2}\dot{x}_1^2$ [thick dashed line]; Energy of oscillator two: $H_2 \equiv \frac{1}{2}\omega_2^2 x_2^2 + \frac{1}{2}\dot{x}_2^2$ [thick continuous line]; Position of oscillator one: x_1 [thin dashed line]; Position of oscillator two: x_2 [thin continuous line].

The study in this chapter started with an interest in getting two coupled conservative nonlinear oscillators to transfer all energy from one oscillator to the other and then back and so on. This can be done with the two coupled linear oscillators

$$\ddot{x}_1 = -\omega_1^2 x_1 + k x_2, \tag{3.1}$$

$$\ddot{x}_2 = -\omega_2^2 x_2 + k x_1, \tag{3.2}$$

where x_1 and x_2 are the positions, ω_1 and ω_2 are constants, and k is a small constant. When $\omega_1 = \omega_2$ with the right initial conditions we get a complete exchange of energy between the two oscillators. We define the energy of each oscillator as $H_i(x_i, \dot{x}_i) \equiv \frac{1}{2}\omega_i^2 x_i^2 + \frac{1}{2}\dot{x}_i^2$, for $i = 1, 2$. So the total energy, $E_T = H_1 + H_2 - k x_1 x_2$, is a constant of the motion.

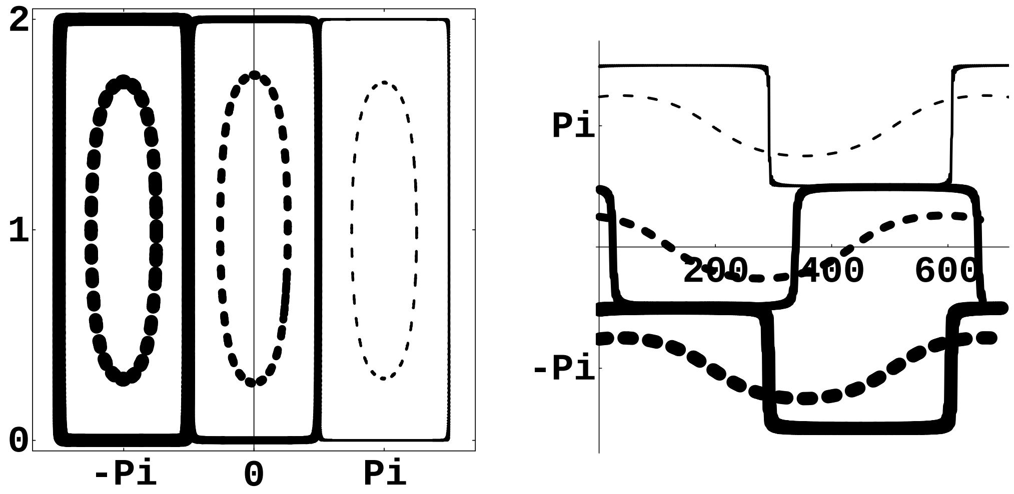

Figure 3.2: Plots of (a) energy, H_2, vs. phase difference, Φ, and (b) Φ vs. t for the two coupled linear oscillators in Eqs.(3.1) and (3.2) with $k = 0.01$ and $\omega_1 = \omega_2 = 1$. $\Phi \equiv \phi_2 - \phi_1$ where ϕ_i is made a continuous function of time by solving for ϕ_i in the expression $x_i = \left(x_i^2 + \frac{\dot{x}_i^2}{\omega_i^2}\right)^{\frac{1}{2}} \cos\phi_i$ where $i = 1, 2$. The six sets of initial conditions all have the same total energy, $E_T = 2$, and $x_1(0) = 0$.

Figs. 3.1 and 3.2 show the following features: There is a complete exchange of energy in the long time span of $\frac{2\pi\omega_1}{k}$; when either one of the oscillators has zero energy there is a quick change in the phase difference, Φ, in a time of approximately $\frac{2\pi}{\omega_1}$; the characteristic resonance circles fill in all the accessible phase space (it's super sized). We will retain these gross features when studying weakly coupled nonlinear oscillators.

In this chapter, we study the same system as in chapter 2 for the case when the angular frequencies of the two oscillators are the same for all values of the energies in the oscillators (intrinsic resonance). To simplify things, we limit our study to just the primary resonance, Eq. (2.4) with $r = s = 1$.

In this chapter, we derive the lowest order standard equations of motion for two coupled oscillators that are at the primary resonance for all initial conditions, then we study this applied to two coupled linear oscillators, and finally we study this when applied to coupled soft and hard Duffing oscillators.

3.1 Equations of Motion at a Super Resonance

We investigate the system of two coupled oscillators of the form

$$\dot{x}_i = \frac{p_i}{m_i}, \tag{3.3}$$

$$\dot{p}_i = F_i(x_i) + \epsilon k x_j, \tag{3.4}$$

$$F_i(x_i) \equiv -\frac{dU_i(x_i)}{dx_i}, \tag{3.5}$$

where $i, j = 1, 2$, $i \neq j$, x_i is a displacement, k and m_i are constants, ϵ is a small constant number, and U_i is the potential of the i-th oscillator. Note that this coupled oscillator system is of the form of the more general coupled oscillator system, Eqs. (2.1)–(2.3), with $k_i \equiv k$, and $\Gamma_i \equiv 0$, where $i = 1, 2$.

Next, we change variables x_i and p_i to their corresponding action-angle variables, J_i and ϕ_i, by using their corresponding transformation functions, $X_i(J_i, \phi_i)$, $P_i(J_i, \phi_i)$, $K_i(J_i)$, and $\omega_i(J_i)$ where $i = 1, 2$, as explained in appendix A.

We will study this system when the primary resonance condition, $\omega_2 = \omega_1$, is satisfied for all time. In order to avoid secular terms, we transform our equations to a rotating frame by using the following change of dynamical variables

$$\Phi \equiv \phi_2 - \phi_1, \tag{3.6}$$

$$K_2(J_2) \qquad \text{as defined previously,} \tag{3.7}$$

$$E_T \equiv K_1 + K_2 - \epsilon k X_1 X_2, \tag{3.8}$$

$$\phi \equiv \phi_1, \tag{3.9}$$

where we refer to E_T as the total energy in the system.

From Eqs. (A.22), (A.40), and (A.41) of appendix A and Eqs. (3.3)–(3.9), the equations of motion of Φ, Ω, I, and ϕ may be written as

$$\dot{\Phi} = \omega_2 - \omega_1 - \epsilon k \frac{\partial X_2}{\partial J_2} X_1 + \epsilon k \frac{\partial X_1}{\partial J_1} X_2, \tag{3.10}$$

$$\dot{K}_2 = \frac{\epsilon k}{m_2} P_2 X_1, \tag{3.11}$$

$$\dot{E}_T = 0, \tag{3.12}$$

$$\dot{\phi} = \omega_1 - \epsilon k \frac{\partial X_1}{\partial J_1} X_2, \tag{3.13}$$

where it is assumed that all quantities on the right side of the equations can be written as functions of just Φ, K_2, E_T, and ϕ. Eqs. (3.10)–(3.13) are exact.

We define a ϕ-averaged function $\langle \xi \rangle_\phi(\Phi, K_2, E_T)$ by

$$\langle \xi \rangle_\phi(\Phi, K_2, E_T) \equiv \frac{1}{2\pi} \int_0^{2\pi} \xi(\Phi, K_2, E_T, \phi)\, d\phi\,. \tag{3.14}$$

In what follows, we use

$$X_i(J_i, \phi_i) = \sum_{l=0}^{\infty} C_{i,l}(J_i) \cos(l\phi_i), \tag{3.15}$$

$$P_i(J_i, \phi_i) = -m_i \omega_i(J_i) \sum_{l=1}^{\infty} l C_{i,l}(J_i) \sin(l\phi_i), \tag{3.16}$$

where $i = 1, 2$.

We approximate the right-hand side of Eqs. (3.10)–(3.13) by the corresponding ϕ-averaged values. This approximation will not be valid when the energy in either oscillator is small, so our calculation will not be quantitatively correct in the regions of phase space where K_2 is close to the total energy or zero energy.

Next we consider the case where the Fourier coefficients $C_{i,l}(J_i)$, as defined in Eqs. (3.15) and (3.16), decrease rapidly with increasing l. So, after averaging we will drop all but the first Fourier harmonics. We will approximate the first Fourier harmonic, $C_{i,1}$, as being equal to the amplitude, A_i, where A_i is defined by $U_i(A_i) \equiv K_i(J_i)$, and $F_i(A_i) < 0$, where $i = 1, 2$.

In addition, we will impose that the average value of $X_i(J_i, \phi_i)$ over ϕ is zero, so that $C_{i,0} = 0$ where $i = 1, 2$. Finally, we assume that the primary resonance condition, $\omega_2 = \omega_1$, is satisfied. This in addition to these two approximations, averaging and then dropping harmonics, gives

$$\dot{\Phi} = \frac{\epsilon k}{2}\omega A_1 A_2 \left(\frac{1}{A_2 F_2(A_2)} - \frac{1}{A_1 F_1(A_1)} \right) \cos\Phi, \tag{3.17}$$

$$\dot{K_2} = -\frac{\epsilon k}{2}\omega A_1 A_2 \sin\Phi, \tag{3.18}$$

where $\omega \equiv \omega_1 = \omega_2$. In order to get an implicit functional dependence of A_1 and on K_2, we will use the approximation that $E_T = K_1 + K_2$. So, we have reduced the original four ODE system to a two ODE system.

Figure 3.3: The general flow of Eqs. (3.17) and (3.18).

The flow of Eqs. (3.17) and (3.18) will be periodic in Φ with a period of 2π. An analysis of Eqs. (3.17) and (3.18) shows that there are four singular points in the flow in the region $0 \le K_2 \le E_T$ and $-\pi < \Phi \le \pi$ as illustrated in Fig. 3.3. There are two regular fixed points at $\Phi = 0, \pi$ at the value of K_2 where $A_2 F_2(A_2) = A_1 F_1(A_1)$. The two regular fixed points will be circle points if

$$\frac{A_2}{F_2(A_2)} \frac{dF_2(A_2)}{dA_2} + \frac{A_1}{F_1(A_1)} \frac{dF_1(A_1)}{dA_1} > 0. \tag{3.19}$$

We do not know of a case where Eq. (3.19) is not satisfied when $\omega_1 = \omega_2$.

3.2 Primer Example: Two Linear Oscillators

For the two coupled linear oscillators, Eqs. (3.1) and (3.2), Eqs. (3.17) and (3.18) may be written as

$$\dot{\Phi} = \frac{k}{2\omega} \left(\frac{\sqrt{K_2}}{\sqrt{E_T - K_2}} - \frac{\sqrt{E_T - K_2}}{\sqrt{K_2}} \right) \cos \Phi, \tag{3.20}$$

$$\dot{K_2} = -\frac{k}{\omega} \sqrt{K_2} \sqrt{E_T - K_2} \sin \Phi. \tag{3.21}$$

Fig. 3.4 illustrates how well this theory shadows the exact dynamics.

3.3 Example: Coupling a Soft and a Hard Duffing Oscillator

We now investigate the two coupled oscillators with the equations of motion

$$\dot{x}_i = p_i, \tag{3.22}$$

$$\dot{p}_i = -a_i x_i - b_i x_i^3 + k x_j, \tag{3.23}$$

where $i, j = 1, 2$, $i \neq j$, a_i[1] is a constant, and b_i and k are small constants. We will make oscillator one ($i = 1$) the soft oscillator. So $b_1 < 0$ and all other constants are greater than zero.

[1] We are running out of symbols. a_i is a different constant then the a_i of chapter 2.

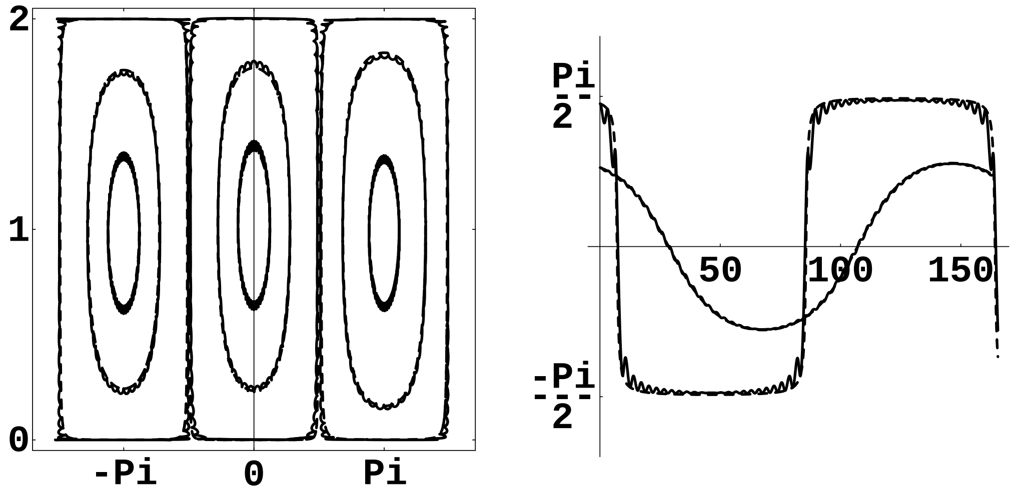

Figure 3.4: Numerical integration of theory, Eqs. (3.20) and (3.21) [dashed lines]. Numerical integration of the exact equations of motion, Eqs. (3.1) and (3.2) [wiggly continuous lines]. Parameter values: $\omega_1 = \omega_2 = \omega = 1$ and $k = 0.04$. The nine sets of initial conditions all have the same total energy, $E_T = 2$, and $x_1(0) = 0$. The two lines are difficult to distinguish at most points.

We define the unperturbed forcing functions to be $F_i(x_i) = -a_i x_i - b_i {x_i}^3$ where $i = 1, 2$. Note that this coupled oscillator system is of the form of the more general coupled oscillator system, Eqs. (3.3) and (3.4), with $m_i = 1$ $(i = 1, 2)$ and $\epsilon k \to k$.

We will use approximate analytic expressions for the angular frequencies, ω_i, $i = 1, 2$, that are valid for $a_i \gg |b_i x_i^2|$. We use the following approximate implicit solution to the corresponding transformation functions, $X_i(J_i, \phi_i)$, $P_i(J_i, \phi_i)$, $K_i(J_i)$, and $\omega_i(J_i)$ $(i = 1, 2)$ from appendix A.

$$X_i(J_i, \phi_i) = A_i \cos\phi_i, \tag{3.24}$$

$$P_i(J_i, \phi_i) = -\omega_i A_i \sin\phi_i, \tag{3.25}$$

$$K_i = \frac{1}{2} a_i A_i^2 + \frac{1}{4} b_i A_i^4, \tag{3.26}$$

$$\omega_i = \sqrt{a_i}\left(1 + \frac{3}{4} b_i K_i\right), \tag{3.27}$$

$$J_i = \frac{K_i}{\sqrt{a_i}}\left(1 + \frac{3}{8} b_i K_i\right). \tag{3.28}$$

To approximately satisfy the primary resonance condition, $\omega_1 = \omega_2$ for all values of the energies K_1 and K_2, we will impose that the force coefficients a_i and b_i satisfy $\omega_1 = \omega_2$ and $E_T = K_1 + K_2$. We introduce the small constant α defined by

$$a_1 = (1+\alpha)^2 , \tag{3.29}$$

$$a_2 = (1-\alpha)^2 , \tag{3.30}$$

so that a_1 and a_2 are both close to 1.

$\omega_1 = \omega_2$, $E_T = K_1 + K_2$, Eq. (3.27) and Eqs. (3.29) and (3.30) give us that

$$(1+\alpha)\left(1+\frac{3}{4}b_1\left(E_T - K_2\right)\right) - (1-\alpha)\left(1+\frac{3}{4}b_2 K_2\right) = 0, \tag{3.31}$$

must be satisfied for all K_2. This gives us

$$b_1 = -\frac{8\alpha}{3E_T(1+\alpha)}, \tag{3.32}$$

$$b_2 = \frac{8\alpha}{3E_T(1-\alpha)}. \tag{3.33}$$

So, if we choose a value for α and the total energy, E_T, we can use Eqs. (3.29) and (3.30), and Eqs. (3.32) and (3.33) to find values of the force coefficients that will cause the two oscillators to exchange all of the energy for some initial conditions.

Eqs. (3.17) and (3.18) can be written for this example with the substitutions

$$\epsilon k \to k, \tag{3.34}$$

$$\omega = \sqrt{a_2}\left(1+\frac{3}{4}b_2 K_2\right), \tag{3.35}$$

$$A_1 = \sqrt{\frac{a_1}{b_1}\left(\sqrt{1+\frac{4b_1\left(E_T - K_2\right)}{a_1^2}} - 1\right)}, \tag{3.36}$$

$$A_2 = \sqrt{\frac{a_2}{b_2}\left(\sqrt{1+\frac{4b_2 K_2}{a_2^2}} - 1\right)}. \tag{3.37}$$

The above equations will be a good approximation for this system in most regions of the phase space if $a_i^2 \gg |b_i E_T|$ and $a_i \gg k$, $i = 1,2$, but in order to make the nonlinearity a larger effect than the coupling, we will impose the inequality $a_i^2 \gg |b_i E_T| \gg k^2$, $i = 1,2$. With the frequency matching conditions, Eqs. (3.32) and (3.33), and assuming that $1 \gg \alpha$, this inequality will be satisfied if $1 \gg \alpha \gg k^2$. From above, the maximum change in the angular frequency of the oscillators will be 2α.

See Fig. 3.5.

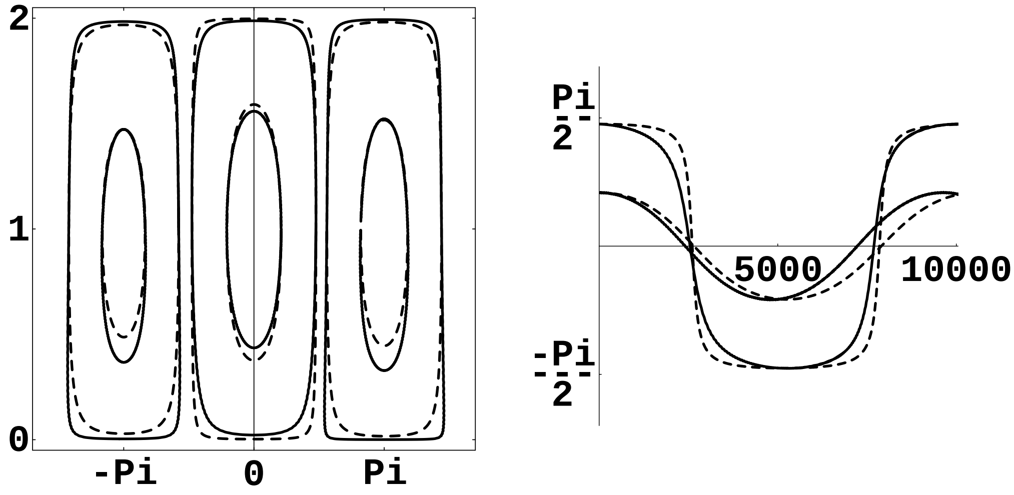

Figure 3.5: Numerical integration of theory, Eqs. (3.17) and (3.18) [dashed lines]. Numerical integration of the exact equations of motion, Eqs. (3.22) and (3.23) [solid lines]. Parameters: $\alpha = 0.02$, $E_T = 2$, and $k = 6 \times 10^{-4}$ with the unperturbed frequencies matched gives $a_1 \approx 1.0404$, $a_2 \approx 0.9604$, $b_1 \approx -0.02614$, and $b_2 \approx 0.02721$.

We see in Fig. 3.5 that our theory and exact solutions do not exactly agree. We attribute the apparent difference to the crude approximation for the transformation functions, Eqs. (3.24)–(3.28).

Fig. 3.6 is a simulation of Eqs. (3.22) and (3.23) with the same parameter values as in Fig. 3.5 except with the values of the force coefficients a_1 set equal to a_2 and b_1 set equal to b_2. Fig. 3.6 shows that the super size resonance island in Fig. 3.5 is not present if the frequency matching condition is not satisfied. The resonance island in Fig. 3.6 is small. We call this resonance an accidental resonance. The values of the angular frequencies just happen to be the same at $K_2 = 1$. More importantly, Fig. 3.6 also shows that the super size resonance in Fig. 3.5 is not just due to the fact that both oscillators are close to linear oscillators. If this were so, Fig. 3.6 would be a super size resonance too.

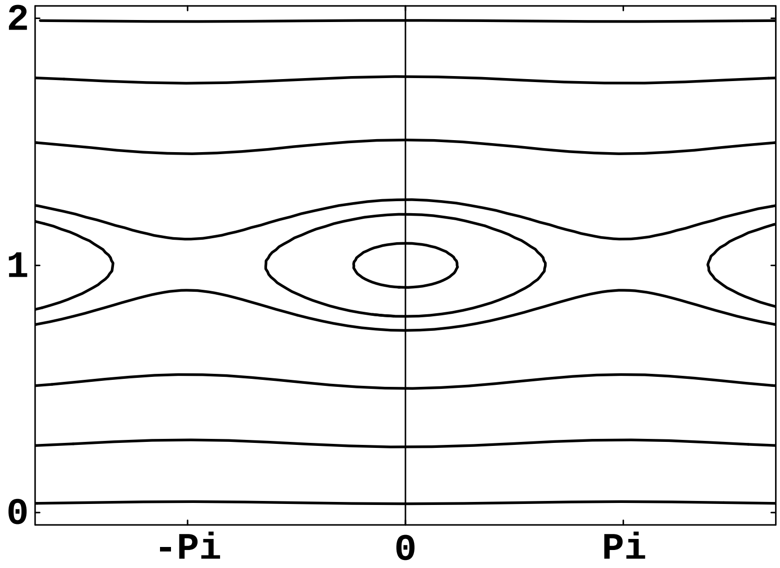

Figure 3.6: Numerical integration of Eqs. (3.22) and (3.23). Parameters: $E_T = 2$ and $k = 6 \times 10^{-4}$, $a_1 = a_2 \approx 0.9604$, and $b_1 = b_2 \approx 0.02721$.

Chapter 4

Frequency Response Curves

A frequency response curve (response curve) for a periodically driven oscillator is a plot of a steady state value of a dynamical variable vs. the frequency or angular frequency of the driving oscillator. We define steady state to be when the position of the driven oscillator has a periodic solution.

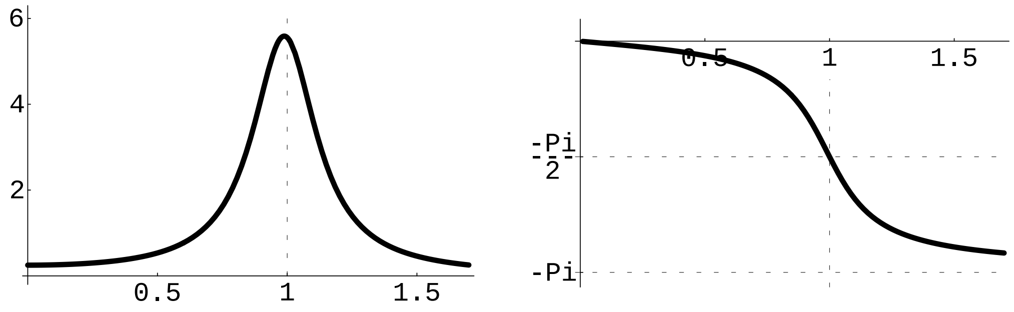

Figure 4.1: Response curves for the system $\ddot{x}_2 = -\omega_2^2 x_2 - \gamma\dot{x}_2 + A_1 \cos\omega_1 t$ with parameter values $\omega_2 = 1$, $A_1 = 1$, and $\gamma = 1$. In (a) $\overline{E_2}$ is the time average of E_2, the energy of the driven oscillator, over the time of a period of the driving oscillator when the system is at steady state. $E_2 \equiv \frac{1}{2}\omega_2^2 x_2^2 + \frac{1}{2}\dot{x}_2^2$. In (b) $\overline{\Phi}$ is the time average of Φ, the phase difference between the driven and the driver oscillators, over the time of a period of the driving oscillator when the system is at steady state. Φ can be defined by the following equations: $\Phi = \phi_2 - \omega_1 t$, $x_2 = A_2 \cos\phi_2$, $E_2 = \frac{1}{2}\omega_2^2 A_2^2$.

The response curves commonly studied for a driven and damped linear oscillator are shown in Fig. 4.1.[1] The analogous plots for a driven nonlinear oscillator are shown in Fig. 4.2.

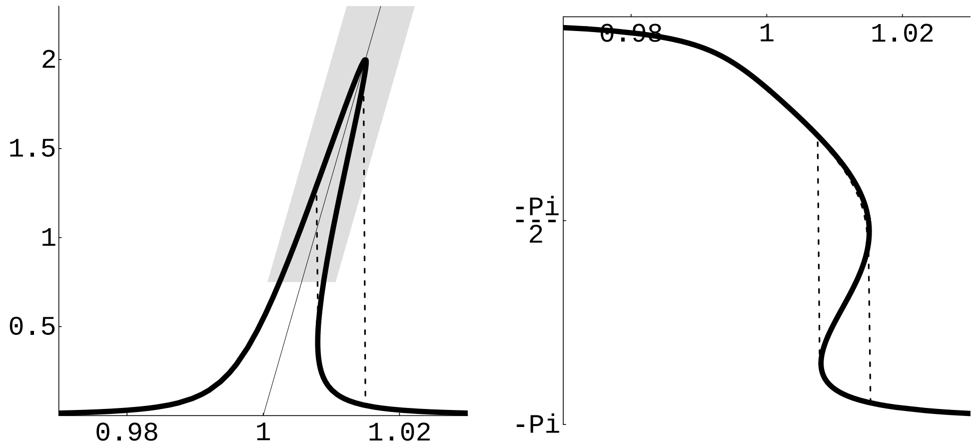

Figure 4.2: Response curves for the system $\ddot{x}_2 = -x_2 - \alpha x_2^3 - \gamma \dot{x}_2 + A_1 \cos \omega_1 t$ with parameter values $\alpha = 0.1$, $A_1 = 0.1$, and $\gamma = 0.05$. In (a) $\overline{E_2}$ is the time average of E_2, the energy of the driven oscillator, over the time of a period of the driving oscillator when the system is at steady state. $E_2 = \frac{1}{2}\omega_2^2 x_2^2 + \frac{1}{2}\dot{x}_2^2$. In (b) $\overline{\Phi}$ is the time average of Φ, the phase difference between the driven and the driver oscillators, over the time of a period of the driving oscillator when the system is at steady state. Φ can be defined by the following equations: $\Phi = \phi_2 - \omega_1 t$, $x_2 = A_2 \cos \phi_2$, $E_2 = \frac{1}{2}\omega_2^2 A_2^2$. The solid lines are from our theory. The dashed lines are from a numerical integration of the equations of motion.

We see that at some values of the driving angular frequency the driven oscillator has several steady state solutions. For instance, at a driving angular frequency of $\omega_1 = 1.01$ we see in Fig. 4.2 that there are three steady state solutions for the time average energy of the driven oscillator, $\overline{E_2}$, and the time average phase difference between the two oscillators, $\overline{\Phi}$. The highest and the lowest of the three points are stable steady state time average energy and phase difference values. The middle point corresponds to an unstable steady state solution, and so the driven oscillator will not sustain this (time average) energy and phase difference value.

[1] As in chapter 2, in this chapter we refer to quantities related to the driver oscillator with a subscript 1 and quantities related to the driven oscillator with a subscript 2.

We call the thin straight line in Fig. 4.2a the backbone of the response curve. The backbone is a plot of the energy vs. the angular frequency, $\omega_2(J_2)$ of the driven oscillator when γ and A_1 are set to zero, where $J_2(E_2)$ is a function of energy E_2.

In chapter 2 section 2.2 we showed that there are only two fixed points in the standard equation that correspond to two steady state periodic solutions of the driven oscillator system. So you are led to the question: "Why are there three steady state solutions at some values of the driving frequency and only two fixed points in the standard equation that correspond to two steady state periodic solutions?" The answer to this question is that the standard equation represents the dynamics of the system near resonance and oscillator energies not near zero, which is in the shaded region of Fig. 4.2a. The lowest $\overline{E_2}$ point at $\omega_1 = 1.01$ in Fig. 4.2a corresponds to the response of the driven oscillator that is driven at a frequency that is not near resonance at this value of the energy $\overline{E_2}$.

Figure 4.3: Energy response curve for the system $\ddot{x}_2 = -x_2 - x_2^3 - \gamma\dot{x}_2 + A_1 \cos\omega_1 t$ with parameter values $\gamma = 0.1$ and $A_1 = 0.1$. The thick solid line is from our first-order theory with the unperturbed oscillator force defined by $F_2(x_2) \equiv -x_2 - x_2^3$ [20]. The thin line is from the first-order method of multiple scales [14] or our method with unperturbed oscillator force defined by $F_2(x_2) \equiv -x_2$. Both of these methods give the same result. The points are from a numerical integration of the exact equation of motion.

Fig.4.3 shows response curves for a sinusoidally driven highly nonlinear oscillator. We see that the response curves calculated by our new method give good results where previously existing methods fail to give good quantitive results.

In this chapter we will derive a first-order perturbative method to calculate response curves for weakly driven and weakly damped nonlinear oscillators. The new thing here is that the driven nonlinear oscillator is not necessarily a weakly nonlinear oscillator.

In this chapter we derive the equation of motion of the energy and phase difference for a general class of driven librating oscillator; then from the fixed points of these equations we find an expression for the response curve, energy vs. driving angular frequency, for this general system; and finally, as a primer example, we apply this method to a sinusoidally driven linear and then weakly nonlinear oscillator.

4.1 The Dynamics Near a Response Curve

We investigate the driven oscillator system of the form

$$\dot{x}_1 = p_1, \tag{4.1}$$

$$\dot{p}_1 = F_1(x_1), \tag{4.2}$$

$$F_1(x_1) \equiv -\frac{dU_1(x_1)}{dx_1}, \tag{4.3}$$

$$U_1(x_1) + \frac{p_1^2}{2} = U_1(A_1), \quad F_1(A_1) < 0, \tag{4.4}$$

$$\dot{x}_2 = \frac{p_2}{m_2}, \tag{4.5}$$

$$\dot{p}_2 = F_2(x_2) + \epsilon\Gamma_2(x_2, p_2) + \epsilon x_1, \tag{4.6}$$

$$F_2(x_2) \equiv -\frac{dU_2(x_2)}{dx_2}, \tag{4.7}$$

where x_1 and p_1 are the variables of the driving oscillator, x_2 and p_2 are the variables of the driven oscillator, A_1, m_1 and m_2 are constants, ϵ is a small constant number, and U_1 and U_2 are the potentials of the corresponding oscillators. We impose the condition Eq. (4.4) so that ϵA_1 is the largest value of the driving force, ϵx_1, in Eq. (4.6). We call ϵA_1 the amplitude of the driving force.

Eqs. (4.1)–(4.7) are of the same form as Eqs.(2.1)–(2.3) with $m_1 = 1$, $k_1 = 0$, $k_2 = 1$, and $\Gamma_1 = 0$. The above equations could have been written in the condensed form $m_2\ddot{x}_2 = F_2(x_2) + \epsilon\Gamma_2(x_2, m_2\dot{x}_2) + \epsilon x_1(t)$, but the above form more easily facilitates the transformation to action-angle variables.

Next, we change variables x_i and p_i to their corresponding action-angle variables, J_i and ϕ_i, by using their corresponding transformation functions, $X_i(J_i, \phi_i)$, $P_i(J_i, \phi_i)$, $K_i(J_i)$, and $\omega_i(J_i)$, where $i = 1, 2$, as explained in appendix A. Then we make the change of variables to J_1, K_2, $\Phi \equiv r\phi_2 - s\phi_1$, and $\phi \equiv \phi_1$, where r and s are integers. The values of r and s are chosen by the resonance condition, Eq. (2.4).

From Eqs. (A.26), (A.40), and (A.41) the equations of motion, Eqs. (4.1)–(4.7), can be written as

$$\dot{J}_1 = 0, \tag{4.8}$$

$$\dot{K}_2 = \frac{\epsilon}{m_2} P_2 \left(\Gamma_2 + X_1\right), \tag{4.9}$$

$$\dot{\Phi} = r\omega_2 - s\omega_1 - \epsilon r \frac{\partial X_2}{\partial J_2} \left(\Gamma_2 + X_1\right), \tag{4.10}$$

$$\dot{\phi} = \omega_1, \tag{4.11}$$

where it is assumed that all quantities on the right side of the equations can be written as functions of just J_1, K_2, Φ, and ϕ. Eqs. (4.8)–(4.11) are exact.

We define a ϕ-averaged function $\langle\xi\rangle_\phi(J_1, K_2, \Phi)$ by

$$\langle\xi\rangle_\phi(J_1, K_2, \Phi) \equiv \frac{1}{2\pi}\int_0^{2\pi} \xi(J_1, K_2, \Phi, \phi)\, d\phi\,. \tag{4.12}$$

We next approximate the right hand side of Eqs. (4.8)–(4.11) by ϕ-averaged values of itself. These ϕ-averaged equations will be a good approximation of the dynamics of the corresponding time averaged values of K_2 and Φ. After this we drop all Φ dependent terms but the terms with the lowest non-zero Fourier harmonics.

These two approximations give

$$\dot{K}_2 = \frac{\epsilon}{m_2}\langle P_2\Gamma_2\rangle_\phi - \frac{\epsilon}{2}\omega_2 C_{1,s}C_{2,r}\sin\Phi, \tag{4.13}$$

$$\dot{\Phi} = r\omega_2 - s\omega_1 - \epsilon r\left\langle \frac{\partial X_2}{\partial J_2}\Gamma_2\right\rangle_\phi - \epsilon r\frac{dC_{2,0}}{dJ_2}C_{1,0} - \frac{\epsilon}{2} r C_{1,s}\frac{dC_{2,r}}{dJ_2}\cos\Phi, \tag{4.14}$$

where all the terms with $\langle\ \rangle_\phi$ just depend on K_2.

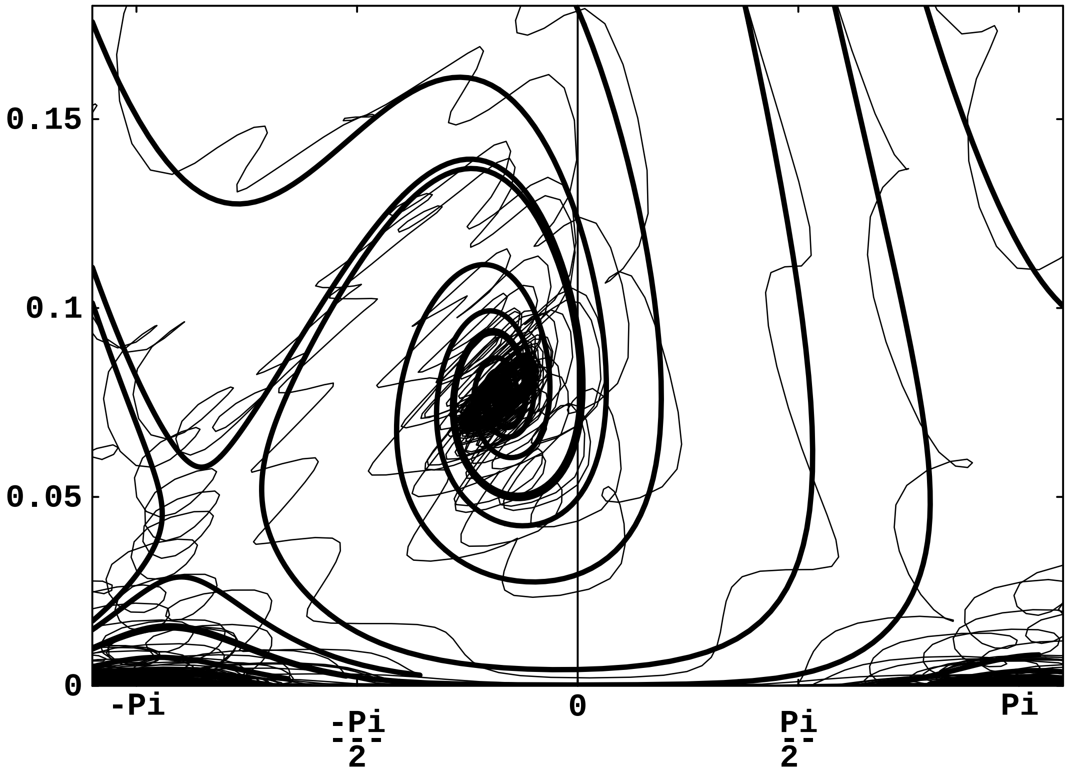

Figure 4.4: Phase plots of K_2 vs. Φ, for the system: $\ddot{x}_2 = -x_2^3 - \gamma \dot{x}_2 + A_1 \cos \omega_1 t$, with parameter values $\gamma = 0.06$, $A_1 = 0.05$, and $\omega_1 = 0.6$. The wiggly lines are from a numerical integration of the exact equation of motion with appropriate definitions of K_2 and Φ (see details in chapter 5). The smooth curves are from a numerical integration of Eqs. (4.13) and (4.14).

Fig. 4.4 shows that there appear to be three fixed points: two focal points and one saddle point. One of the focal points, at about $\Phi \approx \pm\pi$, appears to be pressed against the $K_2 = 0$ boundary. When $K_2 = 0$ the phase angle of the driven oscillator is not defined. As K_2 approaches zero the measured phase angle fluctuates wildly as does K_2. The two focal points correspond to the two stable branches on the over-hanging region of the response curves in Figs. 4.2 and 4.3. The saddle point corresponds to the unstable branch of the response curves.

4.2 General Response Curves

The fixed points of Eqs. (4.13) and (4.14) correspond to the two response curves: E_2 vs. ω_1 and Φ vs. ω_1, where $E_2 = K_2$.[2] The fixed points of Eqs. (4.13) and (4.14) are found by setting $\dot{K}_2$ and $\dot{\Phi}$ to zero and solving for the values of K_2 and Φ.

Doing this gives

$$0 = \frac{1}{m_2}\langle P_2\Gamma_2\rangle_\phi - \frac{r}{2}\omega_2 C_{1,s}C_{2,r}\sin\Phi_f, \tag{4.15}$$

$$0 = r\omega_2 - s\omega_1 - \epsilon r\left\langle \frac{\partial X_2}{\partial J_2}\Gamma_2\right\rangle_\phi - \epsilon r\frac{dC_{2,0}}{dJ_2}C_{1,0} - \frac{\epsilon}{2}rC_{1,s}\frac{dC_{2,r}}{dJ_2}\cos\Phi_f, \tag{4.16}$$

where Φ_f is the fixed-point value of Φ. The value of K_2 that solves Eqs. (4.15) and (4.16) will be denoted as $K_{2,f}$.

Eliminating Φ_f from this expression gives the following equation for the response curve E_2 vs. ω_1

$$\omega_1 = \frac{r}{s}\omega_2\left\{1 - \epsilon\left\langle\frac{\partial X_2}{\partial K_2}\Gamma_2\right\rangle_\phi - \epsilon\frac{dC_{2,0}}{dK_2}C_{1,0} \pm \frac{\epsilon}{2}C_{1,s}\frac{dC_{2,r}}{dK_2}\sqrt{1 - \left(\frac{2\langle P_2\Gamma_2\rangle_\phi}{rm_2\omega_2C_{1,s}C_{2,r}}\right)^2}\right\}, \tag{4.17}$$

where it is assumed that the right hand side of the equation may be written as a function of just Φ_f and $E_{2,f}$ ($E_{2,f} = K_{2,f}$). An analytic expression for the response curve Φ_f vs. ω_1 cannot be written as an equation that is independent of $E_{2,f}$ for this general case.

These results for the values of $E_{2,f}$ and Φ_f are approximately equal to time averaged values of E_2 and Φ, $\overline{E_2}$ and $\overline{\Phi}$, when the driven oscillator is at a steady state.

For the very common case when we have linear damping, $\Gamma_2 = -\gamma\frac{p_2}{m_2}$, and a sinusoidal driving force, $F_1 = -\omega_1^2 x_1$, Eqs. (4.15)–(4.17) can be written as

$$0 = \frac{1}{m_2}\gamma J_2 + \frac{r}{2}A_1C_{2,r}\sin\Phi_f, \tag{4.18}$$

$$0 = r\omega_2 - \omega_1 - \frac{\epsilon}{2}rA_1\frac{dC_{2,r}}{dJ_2}\cos\Phi_f, \tag{4.19}$$

[2] We have many variables that are equal to the energy of the driven oscillator, E_2: $K_2(J_2)$ is the unperturbed Hamiltonian (Kamiltonian) that is a function of action J_2, $H_{2,0}(x_2, p_2) \equiv U_2(x_2) + \frac{p_2^2}{2m_2}$ (from appendix A) is the unperturbed Hamiltonian of the driven oscillator.

$$\omega_1 = r\omega_2 \left\{ 1 \pm \frac{\epsilon}{2} A_1 \frac{dC_{2,r}}{dK_2} \sqrt{1 - \left(\frac{2\gamma J_2}{r m_2 A_1 C_{2,r}} \right)^2} \right\}. \tag{4.20}$$

In this case the approximation of dropping higher harmonics is not necessary. We also note that for this case we are not able to look at resonances with $s \neq 1$, like for example superharmonic resonances, where $s\omega_1 \simeq \omega_2$.

In [21] Nayfeh and Mook show an example in which superharmonic resonances appear at response amplitudes that are of size of order of the driving amplitude. So, this may explain why we are not able to see this effect, because we start with the implied assumption that the driven oscillator amplitude is of size of order 1. It appears that responses to superharmonic resonances are too small for us to see with our method.

4.3 Primer Example: Driven Near Linear Oscillator

As a primer example, we apply this new method of calculating response curves to a driven damped Duffing oscillator with the equations of motion

$$\dot{x}_1 = p_1, \tag{4.21}$$

$$\dot{p}_1 = -\omega_1^2 x_1, \tag{4.22}$$

$$\omega_1^2 x_1^2 + p_1^2 = \omega_1^2 A_1^2, \quad A_1 > 0, \tag{4.23}$$

$$\dot{x}_2 = p_2, \tag{4.24}$$

$$\dot{p}_2 = -\omega_2^2 x_2 - \alpha x_2^3 - \gamma p_2 + x_1, \tag{4.25}$$

where A_1, α, and γ are small constants. Eqs. (4.21)–(4.25) are of the form of Eqs. (4.1)–(4.7) with $F_1 = -\omega_1 x_1$, $F_2 = -\omega_2 x_2$, $\epsilon A_1 \to A_1$, $\epsilon \Gamma_2 = -\alpha x_2^3 - \gamma p_2$, and $m_2 = 1$.

We next change variables x_i and p_i to their corresponding action-angle variables, J_i and ϕ_i, by using their corresponding transformation functions, $X_i(J_i, \phi_i)$, $P_i(J_i, \phi_i)$, $K_i(J_i)$, and $\omega_i(J_i)$ $(i = 1, 2)$ as explained in appendix A. This gives

$$C_{i,l}(J_i) = \delta_{1,l} A_i(J_i), \tag{4.26}$$

$$X_i(J_i, \phi_i) = A_i(J_i) \cos \phi_i, \tag{4.27}$$

$$P_i(J_i, \phi_i) = -\omega_i A_i(J_i) \sin \phi_i, \tag{4.28}$$

$$K_i(J_i) = \frac{1}{2}\omega_i^2 [A_i(J_i)]^2, \tag{4.29}$$

$$A_i(J_i) = \sqrt{\frac{2J_i}{\omega_i}}, \tag{4.30}$$

$$\omega_i(J_i) = \text{constant}, \tag{4.31}$$

where $i = 1, 2$, $\delta_{1,l}$ is the Kronecker delta function, and the amplitude $A_2(J_2)$ is introduced for convenience.

4.3.1 $\alpha = 0$: The Linear Case

Plugging the results of Eqs. (4.26)–(4.31) into Eq. (4.18) and (4.19) with $r = s = 1$ and $\alpha = 0$ and then solving for $E_{2,f}(\omega_1)$ and $\tan \Phi_f(\omega_1)$ gives

$$E_{2,f} = \frac{\frac{1}{2}\omega_2^2 A_1^2}{\left[2\omega_2\left(\omega_2 - \omega_1\right)\right]^2 + \left(\gamma\omega_1\right)^2}, \tag{4.32}$$

$$\tan \Phi_f = \frac{-\gamma\omega_1}{2\omega_2\left(\omega_2 - \omega_1\right)}. \tag{4.33}$$

The exact result for these curves is

$$\overline{E_2} = \frac{\frac{1}{2}\frac{\omega_2^2+\omega_1^2}{2} A_1^2}{\left(\omega_2^2 - \omega_1^2\right)^2 + \left(\gamma\omega_1\right)^2}, \tag{4.34}$$

$$\overline{\Phi} = \frac{\omega_1}{2\pi}\int_{t=0}^{\frac{2\pi}{\omega_1}} \arctan\left[\frac{\frac{\omega_1}{\omega_2}\tan(\omega_1 t + \delta) - \tan(\omega_1 t)}{1 + \frac{\omega_1}{\omega_2}\tan(\omega_1 t + \delta)\tan(\omega_1 t)}\right] dt, \tag{4.35}$$

where $\tan \delta = \frac{\gamma\omega_1}{\omega_1^2 - \omega_2^2}$.

We see that our first-order perturbative method for calculating the response curves does not give the exact results, as may be expected. The relative difference between the two results should be small. The small quantities in this problem are the driving amplitude, A_1, the damping constant, γ; in addition for the ϕ-averaging to be valid the unperturbed angular frequency difference, $\omega_2 - \omega_1$, must be small.[3] We assume that all other parameters are of size of order 1.

[3] In the current literature [3], the small quantity, $\omega_1 - \omega_2$, is commonly called the detuning parameter. However, in our study this quantity is usually not a parameter, but is a dynamical variable because of the action dependence on the angular frequencies.

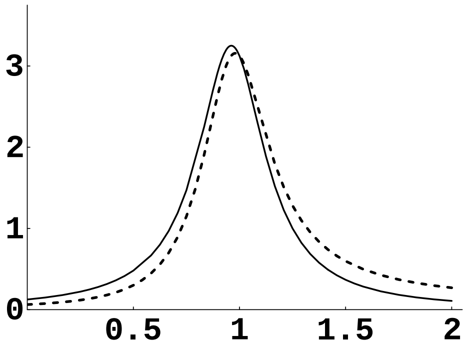

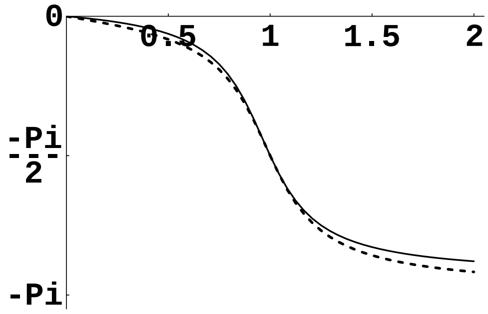

Figure 4.5: Response curves for the linear system in Eqs.(4.21)–(4.25) with parameter values $A_1 = 1$, $\omega_2 = 1$, $\alpha = 0$, and $\gamma = 0.4$. Solid lines are from our theory, Eqs. (4.32) and (4.33) with $K_{2,f} \to \overline{K_2}$ and $\Phi_f \to \overline{\Phi}$. Dotted lines are from the exact response curves, Eqs.(4.34) and (4.35).

From Eq. (4.35) it can be shown that

$$\overline{\Phi} = \delta + \mathcal{O}(\frac{\omega_2 - \omega_1}{\omega_2}), \tag{4.36}$$

where $\mathcal{O}$ is the order function. The leading term in the relative difference between the exact results and our approximate result is

$$\frac{\overline{E_2} - E_{2,f}}{\overline{E_2}} = -\frac{\omega_2 - \omega_1}{\omega_2}\left(1 + \frac{1}{1 + \left(\frac{\gamma}{2(\omega_2 - \omega_1)}\right)^2}\right), \tag{4.37}$$

$$\frac{\overline{\Phi} - \Phi_f}{\overline{\Phi}} = \mathcal{O}(\frac{\omega_2 - \omega_1}{\omega_2}). \tag{4.38}$$

So, we see both these relative differences are small.

Fig. 4.5 is a plot of these responce curves. In these plots we have chosen parameter values and plotting ranges that accentuate the difference between our theory and the exact response curves.

4.3.2 $\alpha \neq 0$: Weakly Nonlinear Case

Plugging the results of Eqs. (4.26)–(4.31) into Eqs. (4.15)–(4.17) gives

$$\gamma A_{2,f} = -\frac{A_1}{\omega_2}\sin\Phi_f, \tag{4.39}$$

$$A_{2,f}(\omega_1-\omega_2) - \frac{3}{8}\frac{\alpha}{\omega_2}A_{2,f}^3 = -\frac{1}{2}\frac{A_1}{\omega_2}\cos\Phi_f, \tag{4.40}$$

$$\omega_1 = \omega_2 + \frac{3}{4}\frac{\alpha}{\omega_2^3}K_{2,f} \pm \frac{A_1}{2\sqrt{2K_{2,f}}}\sqrt{1-K_{2,f}\frac{2\gamma^2}{A_1^2}}, \tag{4.41}$$

where $A_{2,f}$ is the value of A_2 when $K_2 = K_{2,f}$ from Eqs. (4.29) and (4.30). In this case, we are only able to calculate response curves near the primary resonance, $r = s = 1$. This is because both unperturbed oscillators have only one Fourier coefficient. These implicit results for the response curves K_2 vs. ω_1 and Φ vs. ω_1 are the same as when calculated by the method of multiple scales as in Nayfeh and Mook [22]. Fig. 4.2 shows a plot of the response curves for this case.

The point of these primer examples is to show that our method of calculating response curves works well up to first order, as Fig. 4.2 and 4.5 show. In chapter 5 we will show that this new method works equally as well for driven strongly nonlinear oscillators when old methods [3] fail to give good quantitative results.

Chapter 5

Example: Sinusoidally Driven Highly Nonlinear Duffing Oscillator

The following is an example of an application of the methods in chapter 2 and chapter 4 to a specific driven oscillator.

5.1 Change to Action-Angle Variables

We investigate the driven oscillator with the equations of motion

$$\dot{x}_1 = p_1, \tag{5.1}$$

$$\dot{p}_1 = -\omega_1^2 x_1, \tag{5.2}$$

$$\frac{1}{2}\omega_1^2 x_1^2 + \frac{p_1^2}{2} = \frac{1}{2}\omega_1^2 A_1^2, \quad A_1 > 0 \tag{5.3}$$

$$\dot{x}_2 = p_2, \tag{5.4}$$

$$\dot{p}_2 = -{x_2}^3 - \nu x_2 - \gamma p_2 + x_1, \tag{5.5}$$

where ω_1 is a constant and A_1, ν, and γ are small constants.

We define the unperturbed forcing functions to be $F_1(x_1) \equiv -\omega_1^2 x_1$ and $F_2(x_2) \equiv -{x_2}^3$. Note that this coupled oscillator system is of the form of the more general coupled oscillator system, Eqs. (2.1) and (2.2), with $k_1 \equiv 0$, $m_1 \equiv 1$, $m_2 \equiv 1$, $\epsilon k_2 \to 1$, $\Gamma_1 \equiv 0$, and $\epsilon \Gamma_2 \equiv -\nu x_2 - \gamma p_2$.

We next change variables x_i and p_i to their corresponding action-angle variables, J_i and ϕ_i, by using their corresponding transformation functions, $X_i(J_i, \phi_i)$, $P_i(J_i, \phi_i)$, $K_i(J_i)$, and $\omega_i(J_i)$ $(i = 1, 2)$ as explained in appendix A. This gives

$$C_{1,l}(J_1) = \delta_{1,l} A_1(J_1), \tag{5.6}$$

$$X_1(J_1, \phi_1) = A_1(J_1) \cos\phi_1, \tag{5.7}$$

$$P_1(J_1, \phi_1) = -\omega_1 A_1(J_1) \sin\phi_1, \tag{5.8}$$

$$K_1(J_1) = \frac{1}{2}\omega_1^2 [A_1(J_1)]^2, \tag{5.9}$$

$$\omega_1(J_1) = \omega_1, \tag{5.10}$$

$$A_1(J_1) \equiv \sqrt{\frac{2J_1}{\omega_1}} = \text{constant}, \tag{5.11}$$

$$C_{2,l}(J_2) = B_l A_2(J_2), \tag{5.12}$$

$$X_2(J_2, \phi_2) = A_2(J_2) \sum_{l=1}^{\infty} B_l \cos l\phi_2, \tag{5.13}$$

$$P_2(J_2, \phi_2) = -\omega_2(J_2) A_2(J_2) \sum_{l=1}^{\infty} l B_l \sin l\phi_2, \tag{5.14}$$

$$K_2(J_2) = \frac{1}{4}[A_2(J_2)]^4, \tag{5.15}$$

$$\omega_2(J_2) = \rho A_2(J_2), \tag{5.16}$$

$$A_2(J_2) \equiv \sqrt[3]{3\rho J_2}, \tag{5.17}$$

$$\rho \equiv \frac{\pi}{3\sqrt{2}\int_0^1 \sqrt{1 - z^4}dz}, \tag{5.18}$$

where $\delta_{1,l}$ is the Kronecker delta function, B_l are constants, and the amplitude $A_2(J_2)$ is introduced for convenience. The function X_2 can be written as:

$$X_2(J_2, \phi_2) = A_2(J_2)\text{cn}\left(\frac{\phi_2}{\rho}, \frac{1}{\sqrt{2}}\right), \tag{5.19}$$

where cn is the cosine-amplitude Jacobian elliptic function [23]. The first four nonzero values of B_l are approximately 0.9550, 0.04305, 0.001860, and 8.040×10^{-5}, for $l = 1, 3, 5, 7$ respectively. ρ is approximately 0.8472.

5.2 The Standard Equation

With Eqs. (5.6)–(5.18) and Eqs. (2.23)–(2.28) the coefficients of the standard equation for this driven oscillator can be written as

$$a_1 = \frac{\sqrt{2} r^2 \rho^3 \sigma \nu}{\pi \omega_1}, \tag{5.20}$$

$$a_2 = -\frac{r^3 \rho^3 B_r A_1}{2\omega_1^2}, \tag{5.21}$$

$$a_3 = -\frac{\gamma \omega_1}{3}, \tag{5.22}$$

$$a_4 = -\frac{r^3 \rho^3 B_r A_1}{2\omega_1}, \tag{5.23}$$

$$a_5 = -\frac{\gamma}{3}, \tag{5.24}$$

$$a_6 = \frac{r^3 \rho^3 B_r A_1}{2\omega_1^2}, \tag{5.25}$$

where $\sigma \equiv \int_0^1 \frac{dz}{\sqrt[4]{1-z^4}} \approx 1.198$. Therefore, the standard equation, Eqs. (2.20) and (2.21), can be written as

$$\dot{\Phi} = \Omega + \frac{\sqrt{2}\rho^3 r^3 \sigma \nu}{\pi \omega_1} - \frac{r^3 \rho^3 B_r A_1}{2\omega_1^2} \cos \Phi, \tag{5.26}$$

$$\dot{\Omega} = -\frac{\gamma \omega_1}{3} - \frac{r^3 \rho^3 B_r A_1}{2\omega_1} \sin \Phi - \frac{\gamma}{3}\Omega + \frac{r^3 \rho^3 B_r A_1}{2\omega_1^2} \Omega \sin \Phi. \tag{5.27}$$

To show that the dynamics of the standard equation, Eqs. (5.26) and (5.27), are a good representation of the dynamics of the driven oscillator near a resonance, we calculate the values of $\Phi(t)$ and $\Omega(t)$ from the values of $x_i(t)$ and $p_i(t)$, $i = 1, 2$, from a numerical integration of the driven oscillator, Eqs. (5.1)–(5.5), and compare this to values of $\Phi(t)$ and $\Omega(t)$ that we get from the standard equation, Eqs. (5.26) and (5.27). There are three initial conditions needed to integrate Eqs. (5.1)–(5.5): two come from the initial values of Ω and Φ and one comes from setting the initial angle of the driver ϕ_1 to zero.

Fig. 5.1 shows Φ–Ω plane plots with $r = 1$, $\nu = 0$, $A_1 = 1 \times 10^{-2}$, and several values of γ. In Fig. 5.1a we see that with no damping there is no basin of attraction to the phase-locking point. In Fig. 5.1b and Fig. 5.1c we see that with damping there is a basin of attraction to the phase-locking point. In Fig. 5.1d we see a passive resonance; the damping is too large, so there are no fixed points near the resonance.

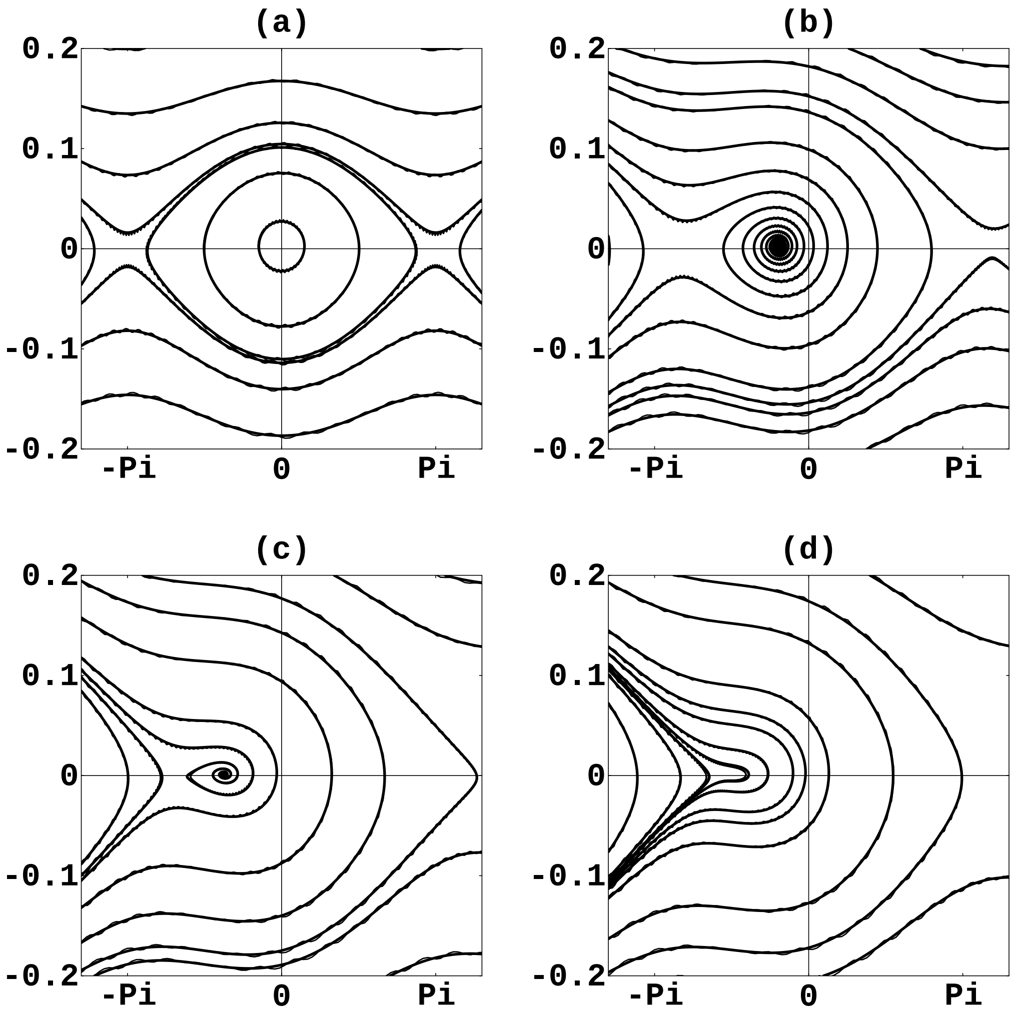

Figure 5.1: The Φ–Ω plane by numerically integrating the standard equation [thick smooth lines] and by computing Φ and Ω from a numerical integration of the exact equations of motion [thin wiggly lines] with $r = 1$, $\omega_1 = 1$, $\nu = 0$, $A_1 = 1 \times 10^{-2}$, and: (a) $\gamma = 0$, (b) $\gamma = 5 \times 10^{-3}$, (c) $\gamma = 8 \times 10^{-3}$, (d) $\gamma = 8.8 \times 10^{-3}$.

To illustrate the effect of a non-zero ν and $r \neq 1$, Fig. 5.2 shows Φ–Ω plane plots with several values of r and ν.

The parameter values used in Fig. 5.2a are the same as those used in Fig. 5.1b except that $\nu = 0$ in Fig. 5.1b and $\nu = 0.05$ in Fig. 5.2a. We see that the effect of nonzero ν is to shift the location of the fixed points in the $-\Omega$ direction and cause larger wiggling about the average.

The parameter values used in Fig. 5.2b are the same as those used in Fig. 5.1b except that $r = 1$ in Fig. 5.1b and $r = 3$ in Fig. 5.2b. In Fig. 5.2b we are looking at a subharmonic resonance. By comparing to Fig. 5.1b we see that the subharmonic of Fig. 5.2b is similar in size and shape but the subharmonic one wiggles more about the average. We are plotting $\Omega = r\rho A_2 - w_1$ on the ordinate. So the size of the change in amplitude, A_2, at the subharmonic resonance is r $(r = 3)$ times smaller than in the primary resonance.

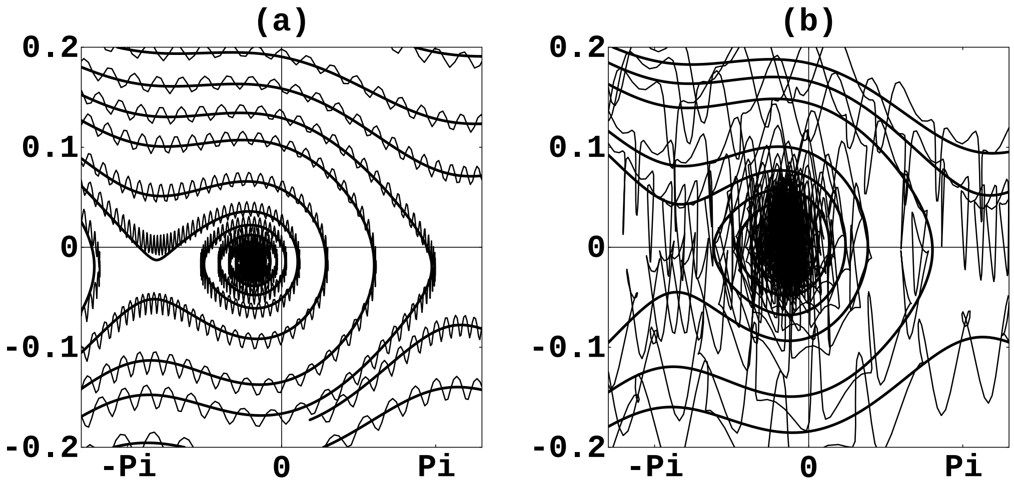

Figure 5.2: The Φ–Ω plane by numerically integrating the standard equation [thick lines] and by computing Φ and Ω from a numerical integration of the exact equations of motion [thin wiggly lines] with $\omega_1 = 1$, $A_1 = 1 \times 10^{-2}$, $\gamma = 5 \times 10^{-3}$, and: (a) $r = 1$, and $\nu = 5 \times 10^{-2}$, (b) $r = 3$, and $\nu = 0$.

5.3 Response Curves

This coupled oscillator system, Eqs. (5.1)–(5.5), is of the form of the more general driven oscillator system, Eqs. (4.1)–(4.7), with $m_2 \equiv 1$, $\epsilon\Gamma_2 \equiv -\nu x_2 - \gamma p_2$, $U_1(x_1) \equiv \frac{1}{2}\omega_1^2 x_1^2$, $U_2(x_2) \equiv \frac{1}{4}x_2^4$, and $\epsilon \to 1$.

Using Eqs. (5.6)–(5.18), Eqs. (4.15)–(4.17) can be written as

$$\sin\Phi_f = -\frac{4\gamma\sqrt{K_{2,f}}}{3\rho B_r A_1}, \tag{5.28}$$

$$\omega_1 = \sqrt{2}r\rho\sqrt[4]{K_{2,f}} + \frac{r\rho^2\sigma\nu}{\pi\sqrt[4]{K_{2,f}}} \pm \frac{r\rho B_r A_1}{4\sqrt{K_{2,f}}}\sqrt{1-\left(\frac{4\gamma\sqrt{K_{2,f}}}{3r\rho B_r A_1}\right)^2}, \tag{5.29}$$

where the ω_1 dependence in Eq. (5.28) comes from the values of $K_{2,f}$ in Eq. (5.29).

With Eqs. (5.28)–(5.29) we can construct accurate response curves for this driven oscillator, as in Figs. 5.3 and 5.4.

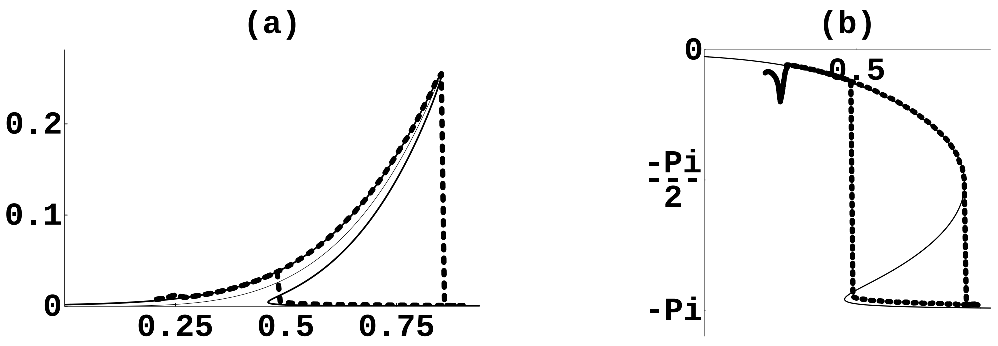

Figure 5.3: Response curves of the driven oscillator of this chapter with parameter values: $\nu = 0.0$, $A_1 = 0.05$, $\gamma = 0.06$. The thick dashed lines are from the exact equations of motion, Eqs. (5.1)–(5.5). The thin solid lines are from our theory, Eqs. (5.28)–(5.29) with $K_{2,f} \to \overline{E_2}$ and $\Phi_f \to \overline{\Phi}$.

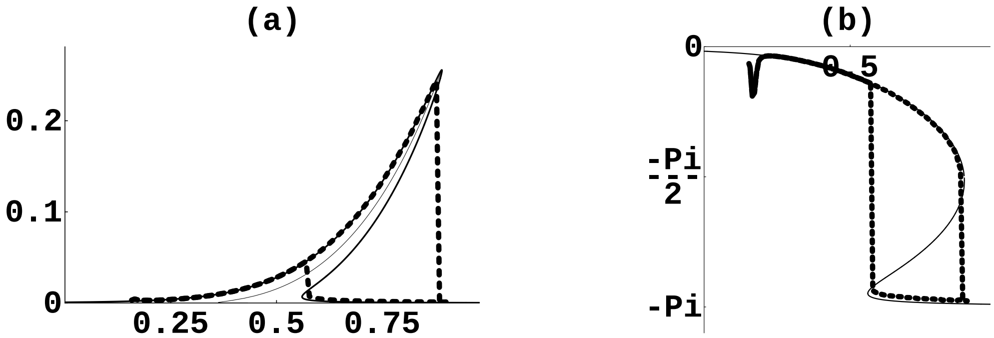

Figure 5.4: Response curves of the driven oscillator of this chapter with parameter values: $\nu = 0.05$, $A_1 = 0.05$, $\gamma = 0.006$. The thick dashed lines are from the exact equations of motion, Eqs. (5.1)–(5.5). The thin solid lines are from our theory, Eqs. (5.28)–(5.29) with $K_{2,f} \to \overline{E_2}$ and $\Phi_f \to \overline{\Phi}$.

Chapter 6

Locking Frequency

This chapter is a continuation of the study of small resonances of chapter 2. We study the local dynamics of two coupled oscillators with two-way coupling near a phase-locking point that is near a resonance. We find the frequency of the motion of the system when it is at this phase-locking point.

Two coupled oscillators are phase-locking when the phase (angle) of one oscillator approaches a rational multiple of the phase of the other oscillator. Two coupled oscillators are phase-locked when the phase of one oscillator is a rational multiple of the phase of the other oscillator.

Fig. 6.1 shows phase space plots of Ω vs. phase difference, Φ, (as defined in chapter 2) for two coupled limit cycle oscillators, from chapter 7. The figures are arranged in a zoom-in sequence from a to d. Fig. 6.1a shows how the phase difference approaches a constant when the oscillators phase-lock. Fig. 6.1b shows how Ω and Φ approach a focal point on an average. In Fig. 6.1c we zoom into the region where the focal point of Fig. 6.1b appears to be, and we see the Φ–Ω dynamics asymptotically approach a periodic limit cycle, in Fig. 6.1d. So, we see the term phase-locking is only an approximate description of this motion. If the two coupled oscillators were to "really" phase-lock, the phase difference of the two oscillators would asymptotically approach a fixed value.

For the case of a driven oscillator, the driven oscillator will always lock to a multiple of the driver oscillator's frequency. For the case of two-way coupling, the locking frequency is not so trivial to calculate. In this chapter we will calculate the locking frequency (angular frequency) to first order. From this point on in this chapter, we will restrict our study to the case of two-way coupling of librating oscillators.

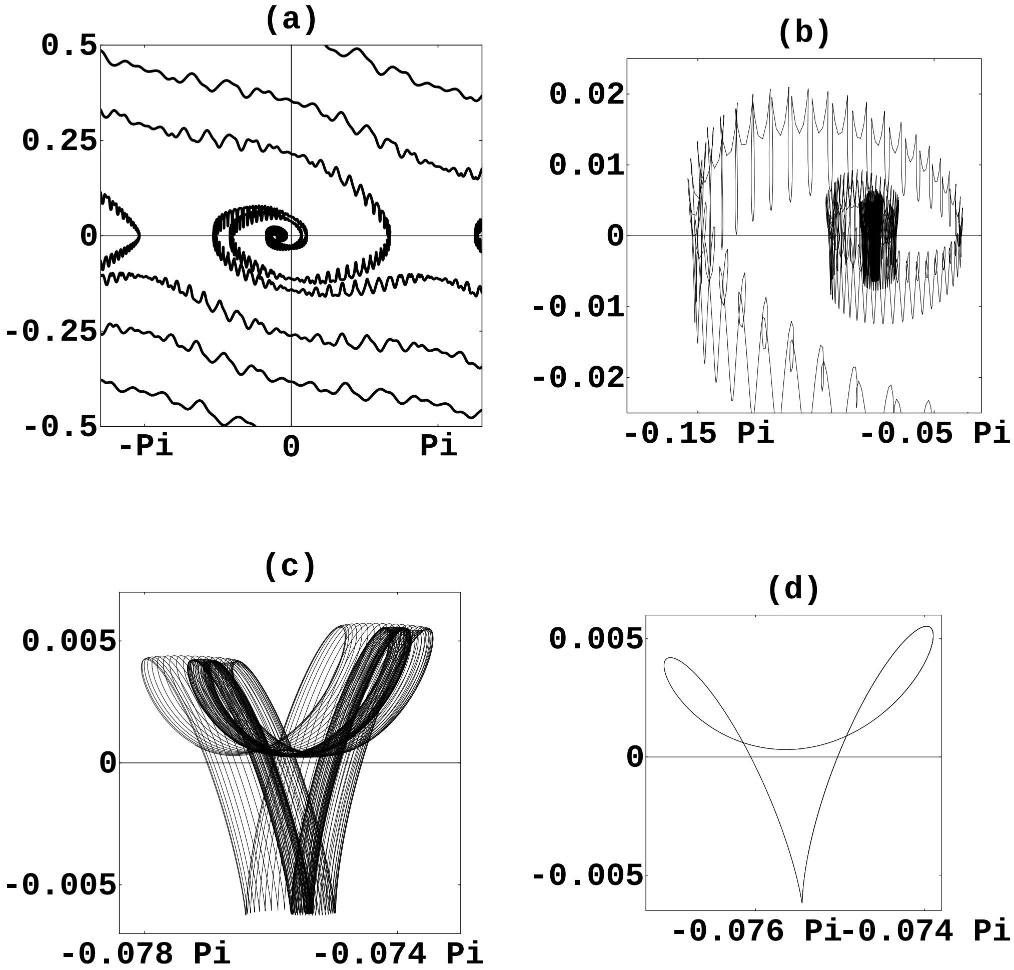

Figure 6.1: A phase plot of Ω vs. Φ from a numerical integration of two coupled limit cycle oscillators, Eqs. (7.1)–(7.4), with parameters: $c_1 = 1$, $b_1 = 1.1$, $\eta_1 = 0.05$, $\eta_2 = 0.05$, $k = 0.01$, $r = 1$, and $s = 1$.

In this chapter we define phase-locking, then we find approximate expressions for the dynamics of the oscillators near a resonance, then we do a linear fixed-point analysis of these equations, and finally we find an approximate expression for the angular frequency of the two coupled oscillators when they are phase-locked.

6.1 What is Locking Frequency?

We assert that when the two oscillators are phase-locked the solution, x_1 and x_2, of the two coupled oscillators, Eqs. (2.1) and (2.2), are periodic functions of t. We refer to these periodic solutions as steady state solutions. The period of this motion, T, can be written as

$$T = \frac{2\pi r}{\overline{\dot{\phi}_1^*}} = \frac{2\pi s}{\overline{\dot{\phi}_2^*}}, \tag{6.1}$$

where $\overline{\dot{\phi}_1^*}$ and $\overline{\dot{\phi}_2^*}$ are time average values of the time derivatives of the angles of the two oscillators when the oscillators are at steady state (phase-locked), and r and s are from the resonance condition, Eq. (2.4). Because of the perturbing forces the exact periods of the two oscillations will be the same. For the case $r \neq 1$ or $s \neq 1$ the exact periods of the motion of the two oscillators will change dramatically even though the motion itself will only be perturbed.

We define the locking angular frequency, ω^*, as

$$\omega^* \equiv \frac{2\pi}{T} = \frac{\overline{\dot{\phi}_1^*}}{r}. \tag{6.2}$$

In order to find an approximate expression for locking angular frequency, first we will find the approximate stable fixed-point values for Φ, Ω, and I, where they satisfy ϕ-averaged equations of motion, Eqs. (6.3)–(6.5). Then we plug these values into the ϕ-averaged value of $\dot{\phi}$, Eq. (2.19), to find the locking angular frequency of the two oscillators.

6.2 Equations of Motion

Since we are interested in the dynamics near phase-locking, we impose that Ω is of order ϵ.[1] In addition we assume that $I - I_0$ is of order ϵ. As in chapter 2, I_0 is defined by the condition $\dot{I}(\Omega = 0, I = I_0) = 0$, where this is the ϕ-averaged value of $\dot{I}$, Eq. (2.18).

Expanding the right side of Eqs. (2.16) – (2.18) about $\Omega = 0$ and $I = I_0$ to first order in Ω and $I - I_0$, and then dropping higher harmonics, as we did in chapter 2, we get

$$\dot{\Phi} = \Omega + a_1 + a_2 \cos\Phi + a_{11}\left(I - I_0\right) + a_{12}\left(I - I_0\right)\cos\Phi, \tag{6.3}$$

$$\dot{\Omega} = a_3 + a_4 \sin\Phi + a_5\Omega + a_6\Omega\sin\Phi + a_7\left(I - I_0\right) + a_8\left(I - I_0\right)\sin\Phi, \tag{6.4}$$

$$\dot{I} = a_9\Omega + a_{10}\left(I - I_0\right), \tag{6.5}$$

where a_i, $i = 1$–12, are constants of size of order ϵ and a_1 through a_6 are given by Eqs. (2.23)–(2.28) and

$$a_9 = \frac{\epsilon r s}{r^2\frac{d\omega_2}{dJ_2} + s^2\frac{d\omega_1}{dJ_1}}\left[\frac{\partial}{\partial J_2}\left(\frac{\langle P_2\Gamma_2\rangle_\phi}{m_2\omega_2}\right) - \frac{\partial}{\partial J_1}\left(\frac{\langle P_1\Gamma_1\rangle_\phi}{m_1\omega_1}\right)\right]\Bigg|_{\Omega=0,I=I_0}, \tag{6.6}$$

$$a_{10} = \frac{\epsilon}{r^2\frac{d\omega_2}{dJ_2} + s^2\frac{d\omega_1}{dJ_1}}\left[s^2\frac{d\omega_1}{dJ_1}\frac{\partial}{\partial J_2}\left(\frac{\langle P_2\Gamma_2\rangle_\phi}{m_2\omega_2}\right) + r^2\frac{d\omega_2}{dJ_2}\frac{\partial}{\partial J_1}\left(\frac{1}{\omega_1}\frac{\langle P_1\Gamma_1\rangle_\phi}{m_1\omega_1}\right)\right]\Bigg|_{\Omega=0,I=I_0} \tag{6.7}$$

where the last step is to evaluate the expressions at $\Omega = 0$ and $I = I_0$. In the above we have used the result that

$$\frac{\partial}{\partial\Omega} = \frac{1}{r^2\frac{d\omega_2}{dJ_2} + s^2\frac{d\omega_1}{dJ_1}}\left(r\frac{\partial}{\partial J_2} - s\frac{\partial}{\partial J_1}\right), \tag{6.8}$$

$$\frac{\partial}{\partial I} = \frac{1}{r^2\frac{d\omega_2}{dJ_2} + s^2\frac{d\omega_1}{dJ_1}}\left(s\frac{d\omega_1}{dJ_1}\frac{\partial}{dJ_2} + r\frac{d\omega_2}{dJ_2}\frac{\partial}{dJ_1}\right), \tag{6.9}$$

which comes from the definitions of Ω and I.[2]

[1] In chapter 2 we imposed that Ω be of order $\epsilon^{\frac{1}{2}}$ when the oscillators are near resonance. Here we want to have all dynamical variables of order of the same distance to the phase-locking point.

[2] We have omitted expressions for expansion coefficients a_7, a_8, a_{11}, and a_{12}. We only need to know that a_7, a_8, a_{11}, and a_{12} are of order ϵ to show that they do not contribute to the subsequent calculations.

6.3 Linear Fixed-Point Analysis

To lowest order in ϵ the fixed points of Eqs. (6.3)–(6.5) satisfy

$$\sin\Phi_f = -\frac{a_3}{a_4}, \tag{6.10}$$

$$\Omega_f = -a_1 - a_2\cos\Phi_f, \tag{6.11}$$

$$I_f = I_0 - \frac{a_9}{a_{10}}\Omega_f, \tag{6.12}$$

where Φ_f, Ω_f, and I_f are the fixed-point values of Φ, Ω, and I respectively. This shows that Φ_f is of size of order 1, and Ω_f and $I_f - I_0$ are both of size of order ϵ as we assumed in section 6.2.

From Eqs. (6.10)–(6.12) to lowest order in ϵ there are two fixed points for Eqs. (6.3)–(6.5) with $0 \le \Phi < 2\pi$ if $|a_4| > |a_3|$, no fixed points if $|a_4| < |a_3|$, and one fixed point if $|a_4| = |a_3|$.

Linearizing Eqs. (6.3)–(6.5) about the fixed points Φ_f, Ω_f, and I_f gives

$$\begin{bmatrix} \dot{\Delta\Phi} \\ \dot{\Delta\Omega} \\ \dot{\Delta I} \end{bmatrix} = \begin{bmatrix} \frac{a_2a_3}{a_4} & 1 & a_{11} + a_{12}\cos\Phi_f \\ \left(a_4 + a_6\Omega_f - \frac{a_8a_9}{a_{10}}\Omega_f\right)\cos\Phi_f & a_5 - \frac{a_3a_6}{a_4} & a_7 - \frac{a_3a_8}{a_4} \\ 0 & a_9 & a_{10} \end{bmatrix} \begin{bmatrix} \Delta\Phi \\ \Delta\Omega \\ \Delta I \end{bmatrix}, \tag{6.13}$$

where

$$\Delta\Phi \equiv \Phi - \Phi_f, \tag{6.14}$$

$$\Delta\Omega \equiv \Omega - \Omega_f, \tag{6.15}$$

$$\Delta I \equiv I - I_f. \tag{6.16}$$

From Eq. 6.13 the three characteristic exponents, λ ($\Delta\Phi$, $\Delta\Omega$, $\Delta I \sim e^{\lambda t}$), must satisfy

$$\begin{aligned} & \lambda^3 - \left[\tfrac{a_2a_3}{a_4} + a_5 - \tfrac{a_3a_6}{a_4} + a_{10}\right]\lambda^2 \\ + \quad & \left[\left(\tfrac{a_2a_3}{a_4}\right)\left(a_5 - \tfrac{a_3a_6}{a_4}\right) - \left(a_4 + a_6\Omega_f - \tfrac{a_8a_9}{a_{10}}\Omega_f\right)\cos\Phi_f \right. \\ & \left. + \tfrac{a_2a_3}{a_4}a_{10} + \left(a_5 - \tfrac{a_3a_6}{a_4}\right)a_{10} - \left(a_7 - \tfrac{a_3a_8}{a_4}\right)a_9\right]\lambda \\ - \quad & \tfrac{a_2a_3}{a_4}\left(a_5 - \tfrac{a_3a_6}{a_4}\right)a_{10} + \tfrac{a_2a_3}{a_4}\left(a_7 - \tfrac{a_3a_8}{a_4}\right)a_9 + \left(a_4 + a_6\Omega_f - \tfrac{a_8a_9}{a_{10}}\Omega_f\right)a_{10}\cos\Phi_f \\ - \quad & \left(a_4 + a_6\Omega_f - \tfrac{a_8a_9}{a_{10}}\Omega_f\right)(a_{11} + a_{12}\cos\Phi_f)\,a_9\cos\Phi_f \quad = \quad 0\,. \end{aligned} \tag{6.17}$$

An analytic solution for λ in Eq. (6.17) can be found in general. We, however, will examine this solution to the lowest order in ϵ.

To the lowest order in ϵ Eq. (6.17) can be approximated by

$$\lambda^3 - \left(\frac{a_2 a_3}{a_4} + a_5 - \frac{a_3 a_6}{a_4} + a_{10}\right)\lambda^2 - (a_4 \cos\Phi_f)\,\lambda + a_4 a_{10}\cos\Phi_f = 0. \tag{6.18}$$

This shows us that when we are close to the fixed points, to lowest order in ϵ, we may ignore the coefficients a_7, a_8, a_{11}, and a_{12}. The fixed point location of I, Eq. (6.12), depends on a_9, so we will keep it even though it does not appear in Eq. (6.18). Then Eq. (6.13) may by written as

$$\begin{bmatrix} \dot{\Delta\Phi} \\ \dot{\Delta\Omega} \\ \dot{\Delta I} \end{bmatrix} = \begin{bmatrix} \frac{a_2 a_3}{a_4} & 1 & 0 \\ a_4\cos\Phi_f & a_5 - \frac{a_3 a_6}{a_4} & 0 \\ 0 & a_9 & a_{10} \end{bmatrix} \begin{bmatrix} \Delta\Phi \\ \Delta\Omega \\ \Delta I \end{bmatrix}. \tag{6.19}$$

So, when we are close to the fixed points, Φ and Ω evolve independently of I as we asserted in chapter 2 for a larger region of the phase space.

The results in chapter 2 section 2.2 discuss the location and local behavior of the phase-locking point in the Φ–Ω plane. From this we see that in order for the phase-locking to be stable, the phase-locking fixed point must be a stable focal point in the Φ–Ω plane. In addition, the fixed point must be stable in the I direction, which from Eq. (6.19) implies that a_{10} must be less then zero.

6.4 Locking Frequency

By using the above and Eq. (2.19) we approximate locking angular frequency, ω^*, as

$$\begin{aligned} \omega^* = \frac{1}{r}&\left[\omega_1 - \epsilon\left\langle \frac{\partial X_1}{\partial J_1}\Gamma_1\right\rangle_\phi - \epsilon k_1 \frac{dC_{1,0}}{dJ_1}C_{2,0} - \frac{\epsilon k_1}{2}\frac{dC_{1,s}}{dJ_1}C_{2,r}\cos\Phi_f\right]\Bigg|_{\Omega=0,I=I_0} \\ &+ \left[\frac{\frac{d\omega_1}{dJ_1}}{r^2\frac{d\omega_2}{dJ_2} + s^2\frac{d\omega_1}{dJ_1}}\right]\Bigg|_{\Omega=0,I=I_0}\left(\left[\frac{d\omega_2}{dJ_2}\right]\Bigg|_{\Omega=0,I=I_0}(I_f - I_0) - \frac{s}{r}\Omega_f\right). \end{aligned} \tag{6.20}$$

We will use this expression to calculate the locking angular frequency of two coupled limit cycle oscillators in chapter 7.

The time dependence of ω^* near the phase-locking can be found from the above expression by substituting time-dependent forms of Ω and I near phase-locking, for Ω_f and I_f respectively.

Chapter 7

Example: Coupled Highly Nonlinear Duffing Van Der Pol Oscillators

Following is an example of an application of the methods of chapter 2 and chapter 6 to two coupled limit cycle oscillators near resonance.

7.1 Change to Action-Angle Variables

We investigate two coupled oscillators with the dimensionless equations of motion [24]

$$\dot{x}_1 = p_1, \tag{7.1}$$

$$\dot{p}_1 = -c_1 x_1^3 + \eta_1 (b_1 - x_1^2) p_1 + k x_2, \tag{7.2}$$

$$\dot{x}_2 = p_2, \tag{7.3}$$

$$\dot{p}_2 = -x_2^3 + \eta_2 (1 - x_2^2) p_2 + k x_1, \tag{7.4}$$

where c_1 and b_1 are constants, and η_1, η_2, and k are small constants. We will impose that all these constants are greater than or equal to zero. We define the unperturbed forcing functions to be $F_1(x_1) \equiv -c_1 x_1^3$ and $F_2(x_2) \equiv -x_2^3$. Note that this coupled oscillator system is of the form of Eqs. (2.1) and (2.2) in chapter 2 with $m_1 = 1$, $m_2 = 1$, $\epsilon k_1 \equiv k$, $\epsilon k_2 = k$, $\epsilon \Gamma_1 \equiv \eta_1 (b_1 - x_1^2) p_1$, and $\epsilon \Gamma_2 \equiv \eta_2 (1 - x_2^2) p_2$.

Next we change variables x_i and p_i to their corresponding action-angle variables, J_i and ϕ_i, by using their corresponding transformation functions, $X_i(J_i,\phi_i)$, $P_i(J_i,\phi_i)$, $K_i(J_i)$, and $\omega_i(J_i)$ $(i=1,2)$ as explained in appendix A. This gives

$$C_{1,l}(J_1) = B_l A_1(J_1), \tag{7.5}$$
$$X_1(J_1,\phi_1) = A_1(J_1)\sum_{l=1}^{\infty} B_l \cos l\phi_1, \tag{7.6}$$
$$P_1(J_1,\phi_1) = -\omega_1(J_1)A_1(J_1)\sum_{l=1}^{\infty} lB_l \sin l\phi_1, \tag{7.7}$$
$$K_1(J_1) = \frac{1}{4}c_1[A_1(J_1)]^4, \tag{7.8}$$
$$\omega_1(J_1) = \sqrt{c_1}\rho A_1(J_1), \tag{7.9}$$
$$A_1(J_1) = \frac{\sqrt[3]{3\rho J_1}}{\sqrt[6]{c_1}}, \tag{7.10}$$
$$C_{2,l}(J_2) = B_l A_2(J_2), \tag{7.11}$$
$$X_2(J_2,\phi_2) = A_2(J_2)\sum_{l=1}^{\infty} B_l \cos l\phi_2, \tag{7.12}$$
$$P_2(J_2,\phi_2) = -\omega_2(J_2)A_2(J_2)\sum_{l=1}^{\infty} lB_l \sin l\phi_2, \tag{7.13}$$
$$K_2(J_2) = \frac{1}{4}[A_2(J_2)]^4, \tag{7.14}$$
$$\omega_2(J_2) = \rho A_2(J_2), \tag{7.15}$$
$$A_2(J_2) = \sqrt[3]{3\rho J_2}, \tag{7.16}$$
$$\rho \equiv \frac{\pi}{3\sqrt{2}\int_0^1 \sqrt{1-z^4}dz}, \tag{7.17}$$

where B_l and ρ are the same constants as in section 5.1. The amplitudes $A_1(J_1)$ and $A_2(J_2)$ are introduced for convenience.

7.2 The Standard Equation

With Eqs. (7.5)–(7.17) and Eqs. (2.23)–(2.28) the coefficients of the standard equation for this coupled oscillator system can be written as

$$a_1 = 0, \tag{7.18}$$

$$a_2 = -\frac{\rho B_r B_s k}{2rs^2 c_1 A_{1,0}} \left(r^4 - s^4 c_1 \right), \tag{7.19}$$

$$a_3 = s\rho\sqrt{c_1}\eta_1\eta_2 A_{1,0} \frac{\left(r^2 - s^2 b_1 c_1\right)\left(r^4 + s^4 c_1\right)}{3\left(r^6\eta_1 + s^6 c_1^2 \eta_2\right)}, \tag{7.20}$$

$$a_4 = -\frac{\rho^2 B_r B_s k}{2rs\sqrt{c_1}} \left(r^4 + s^4 c_1 \right), \tag{7.21}$$

$$a_5 = \frac{1}{3}\,\frac{1}{r^4 + s^4 c_1}\left[r^4\eta_2 + s^4 b_1 c_1 \eta_1 - \frac{9\sqrt{2}}{\pi}\rho\varrho c_1 A_{1,0}^2 \left(s^4\eta_1 + r^2 s^2 \eta_2 \right) \right], \tag{7.22}$$

$$a_6 = \frac{\rho B_r B_s k}{2rs^2 c_1 A_{1,0}} \left(r^4 - s^4 c_1 \right), \tag{7.23}$$

$$A_{1,0} \equiv \sqrt{\frac{\pi}{3\sqrt{2}\rho\varrho}\,\frac{r^6 b_1 \eta_1 + r^2 s^4 c_1 \eta_2}{r^6\eta_1 + s^6 c_1^2 \eta_2}}, \tag{7.24}$$

$$\varrho \equiv \int_0^1 z^2\sqrt{1 - z^4}\,dz. \tag{7.25}$$

$A_{1,0}$ is the value of the amplitude, A_1, that satisfies $\dot{I} = 0$ and the resonance condition, $r\omega_2 = s\omega_1$, where $\dot{I}$ is represented by the ϕ-averaged value of $\dot{I}$ in Eq. (2.18). ϱ is approximately equal to 0.2396.

The standard equation, Eqs. (2.20) and (2.21), for this two coupled oscillator system is

$$\dot{\Phi} = \Omega + a_2 \cos\Phi, \tag{7.26}$$

$$\dot{\Omega} = a_3 + a_4 \sin\Phi + a_5\Omega + a_6\Omega\sin\Phi, \tag{7.27}$$

where the a_i, $i = 2, 3, 4, 5, 6$, is defined in Eqs. (7.18)–(7.24).

To show that the dynamics of the standard equation, Eqs. (7.26) and (7.27), are a good representation of the dynamics of this two coupled oscillator system near a resonance, we calculate the values of $\Phi(t)$ and $\Omega(t)$ from the values of $x_i(t)$ and $p_i(t)$, $i = 1, 2$, from a numerical integration of Eqs. (7.1)–(7.4), and compare this to values of $\Phi(t)$ and $\Omega(t)$ that we get from the standard equation, Eqs. (7.26) and (7.27).

There are four initial conditions necessary to integrate Eqs. (7.1)–(7.4), two come from the initial values of Ω and Φ, one comes from the condition $I(t = 0) = I_0$, and the last comes from setting the initial value of ϕ_1 equal to zero.

Fig. 7.1 shows how the Φ–Ω phase plot changes as the parameter c_1 is changed. In Fig. 7.1a the two oscillators are identical and all initial conditions are attracted to the phase-locking point. In Figs. 7.1b and 7.1c, c_1 is increased and the size of the basin of attraction to the phase-locking point gets smaller. In Fig. 7.1d, we have a passive resonance; c_1 is so large that there are no fixed points near the resonance.

Fig. 7.2 shows how the Φ–Ω phase plot changes as the several parameters are changed.

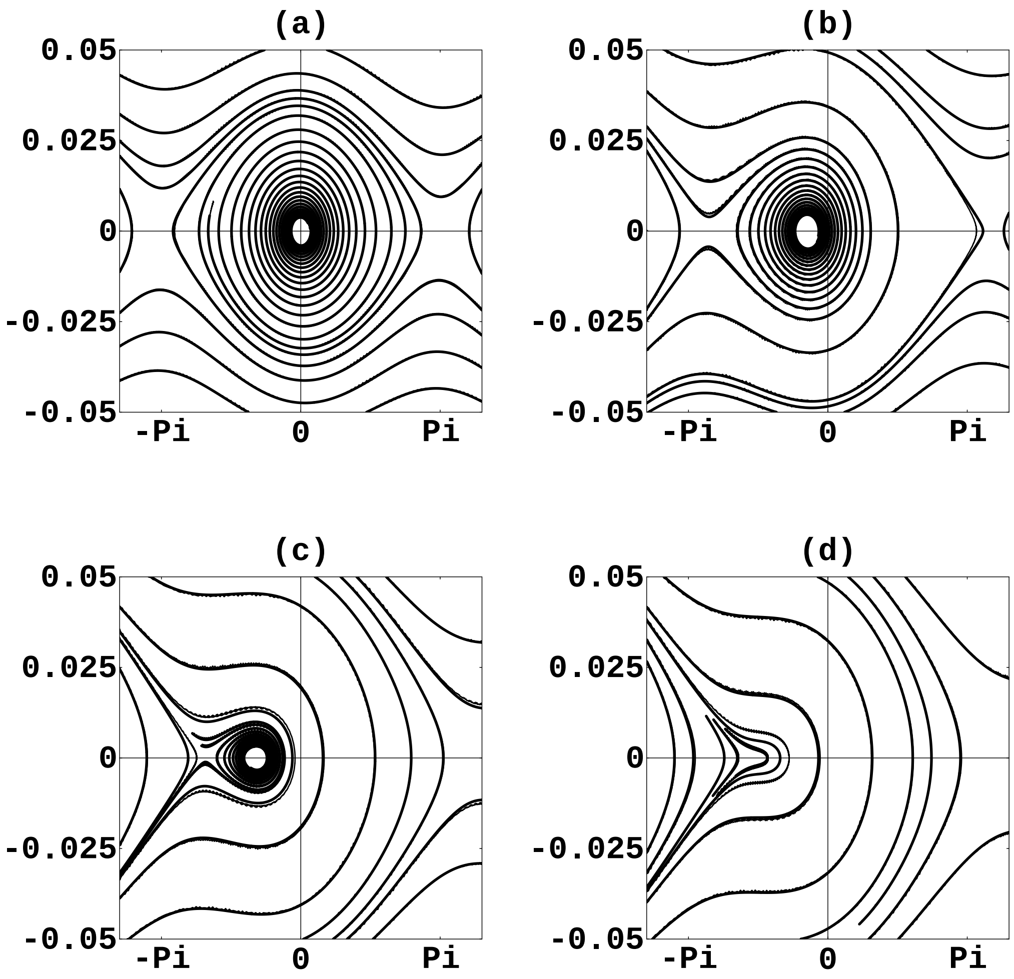

Figure 7.1: The Φ–Ω plane by numerically integrating the standard equation [thick smooth lines] and by computing Φ and Ω from a numerical integration of the exact equations of motion [thin wiggly lines] with $r = 1$, $s = 1$, $b_1 = 1$, $\eta_1 = \eta_2 = 1 \times 10^{-3}$, $k = 5 \times 10^{-4}$, and: (a) $c_1 = 1$, (b) $c_1 = 1.3$, (c) $c_1 = 1.7$, (d) $c_1 = 2$.

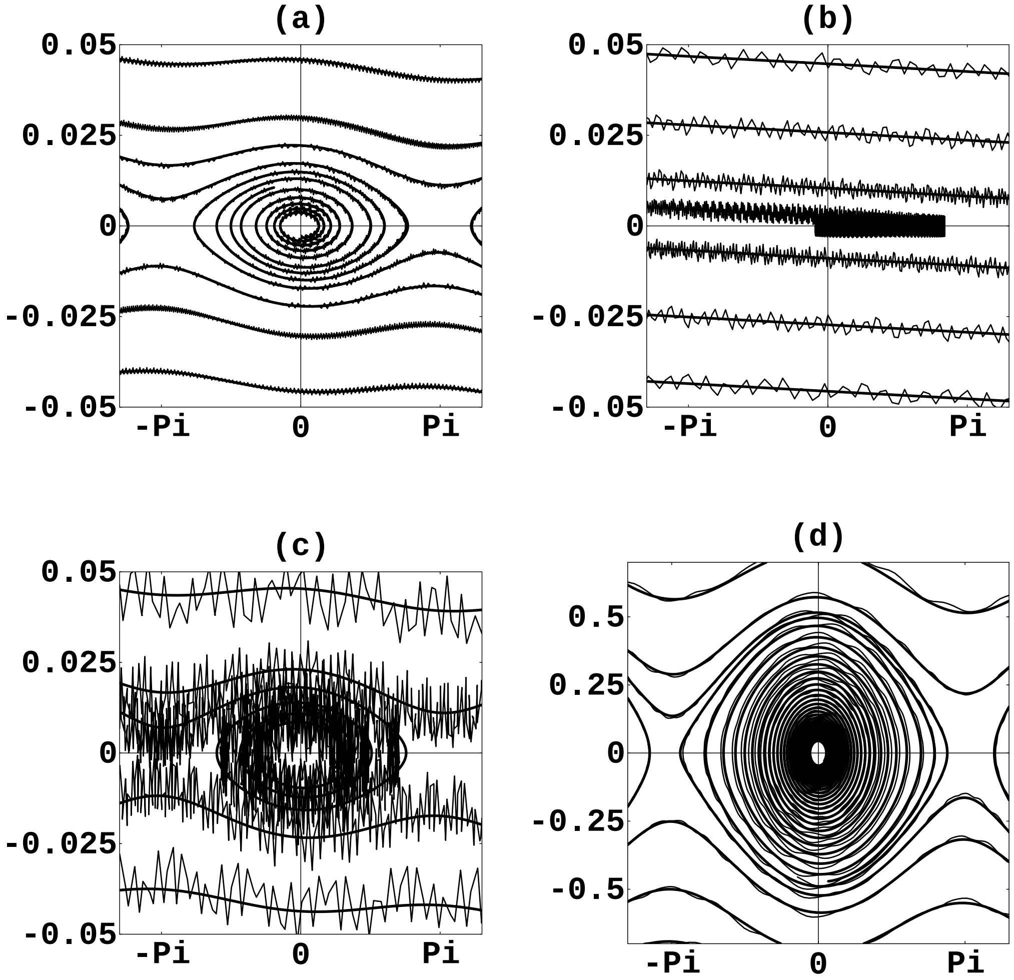

Figure 7.2: The Φ–Ω plane by numerically integrating the standard equation [thick smooth lines] and by computing Φ and Ω from a numerical integration of the exact equations of motion [thin wiggly lines]. Most parameter values for the figures are the same. The parameters are $r = 1$, $s = 1$, $b_1 = 1$, $\eta_1 = \eta_2 = 1 \times 10^{-3}$, $k = 5 \times 10^{-4}$, $c_1 = 1$, $b_1 = 1$, except in: (a) $r = 3$, $c_1 = 9$, (b) $r = 3$, $s = 5$, $c_1 = 0.35$, (c) $s = 5$, $c_1 = 0.4$, (d) $\eta_1 = \eta_2 = 0.01$, $k = 0.1$.

7.3 Locking Frequency

From Eqs. (6.10)–(6.12), Eq. (6.20), and Eqs. (7.18)–(7.24) the expected locking frequency for this system is

$$\omega^* = \frac{\rho}{r}\sqrt{c_1}A_{1,0} - \left(\frac{s\rho B_r B_s k}{2r^2 A_{1,0}} - \frac{a_2}{r}\,\frac{r^3\frac{\rho^2 a_9}{A_{1,0}^2 a_{10}} + s^3 c_1}{r^4 + s^4 c_1}\right)\sqrt{1-\left(\frac{a_3}{a_4}\right)^2}, \tag{7.28}$$

$$a_9 = \frac{1}{\rho^2}\,\frac{s^3 c_1}{r^4 + s^4 c_1}\left[rA_{1,0}^2\left(-b_1\eta_1 + \eta_2\right) + \frac{5\sqrt{2}}{r\pi}\rho\varrho A_{1,0}^4\left(r^2\eta_1 - s^2 c_1\eta_2\right)\right], \tag{7.29}$$

$$a_{10} = -\frac{2}{3}\,\frac{r^4 b_1\eta_1 + s^4 c_1\eta_2}{r^4 + s^4 c_1}. \tag{7.30}$$

a_{10} must be less than zero for the phase-locking to be stable, as stated in section 6.3. Eq. (7.30) shows that this is so for all valid parameter values. So, from section 2.2, phase-locking will be possible if $|a_4| > |a_3|$.

Fig. 7.3 shows that the locking frequency as given in Eq. (7.28) is in excellent agreement with a locking frequency calculated from a numerical integration of the exact equations of motion, Eqs. (7.1)–(7.4).

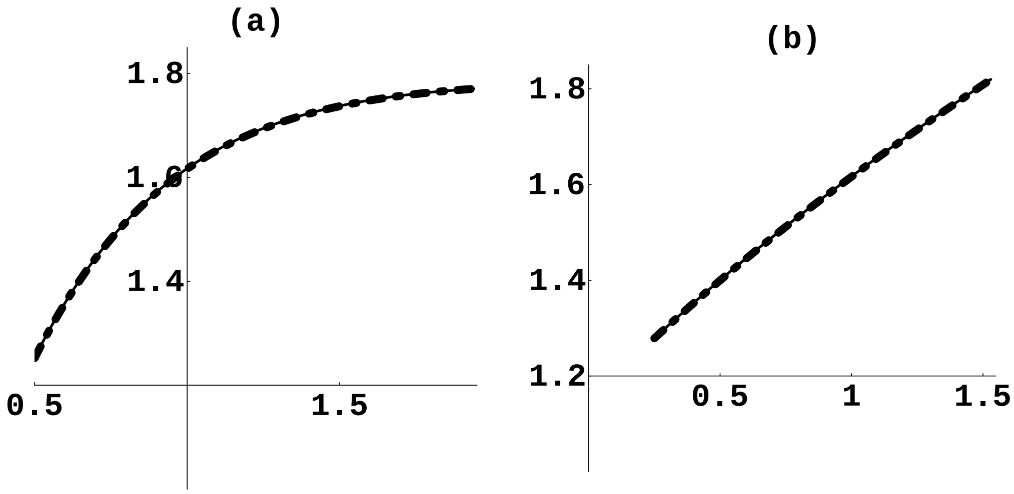

Figure 7.3: Locking angular frequency, ω^*, as a function of (a) c_1 and (b) b_1. The dashed line is from a numerical integration of the exact equations of motion, Eqs. (7.1)–(7.4). The thin continuous line is from our theory, Eq. (7.28). The nonvarying parmeters were: $r = 1$, $s = 1$, $b_1 = 1$, $c_1 = 1$, $\eta_1 = \eta_2 = 0.01$, and $k = 0.005$.

Chapter 8

Concluding Remarks

8.1 Summary of Results

We have studied the dynamics of two conservative librating oscillators with perturbations from a linear displacement coupling and non-Hamiltonian forces such as damping.

In chapter 2, we showed that near an accidental resonance a large class of driven oscillators and two coupled oscillators, Eqs. (2.1)–(2.3), can be transformed to the same ODEs that we call the standard equation: $\dot{\Phi} = \Omega + a_1 + a_2 \cos\Phi$, $\dot{\Omega} = a_3 + a_4 \sin\Phi + a_5\Omega + a_6\Omega\sin\Phi$, where the constants a_4 and a_5 are weighted sums and a_1, a_2, a_3, and a_6 are weighted differences, which depend on Fourier coefficients and frequencies of the unperturbed oscillators and their derivatives with respect to action. a_2, a_4, and a_6 are directly proportional to the coupling constant. a_1, a_3, and a_5 are directly proportional to other constant factors as they appear in the non-coupling perturbing forces (such as damping). The two variables Φ and Ω are defined by: $\Phi \equiv r\phi_2 - s\phi_1$ and $\Omega \equiv r\omega_2(J_2) - s\omega_1(J_1)$, where J_1, J_2, ϕ_1, and ϕ_2 are the corresponding action-angle variables, r and s are integers, and $\omega_2(J_2)$ and $\omega_1(J_1)$ are functionally the same as the angular frequencies of the two uncoupled conservative oscillators.

We showed that if $a_4 > a_3$ then there is a focal point and a saddle point in the Φ–Ω phase space in $0 \leq \Phi < 2\pi$. Then if the real part of the characteristic exponents, λ_i, is less than zero, $\frac{1}{2}\left(\frac{a_3 a_2}{a_4} + a_5 - \frac{a_3 a_6}{a_4}\right) < 0$, then the focal point will be a stable phase-locking point. If in addition, $a_4 \gg a_3$ (i.e., damping forces are small compared to coupling) the phase difference, Φ, at the phase-locking point depends only on the sign of the nonlinearity parameter G, where $G \equiv \left(\frac{\partial \omega_1}{\partial J_1} + \frac{\partial \omega_2}{\partial J_2}\right)\Big|_{\Omega=0, e=e_0}$ for two coupled oscillators. This leads to the result that two hard oscillators ($G > 0$) lock in phase and two soft oscillators ($G < 0$) lock out of phase.

For the case of two coupled damped identical oscillators we showed that the dynamics near the primary resonance, the standard equation, is that of a damped pendulum, $\dot{\Phi} = \Omega$, $\dot{\Omega} = a_4 \sin \Phi + a_5 \Omega$.

In chapter 3 we studied a general system of two coupled conservative oscillators at an intrinsic resonance. We showed in an example that we can find parameters to match the frequencies of a soft Duffing oscillator and a hard Duffing oscillator. We showed that with these two oscillators coupled together for some initial conditions the two oscillators will completely exchange energy back and forth, like two coupled linear oscillators, but with the frequency of the oscillators changing as they swap energy.

In chapter 4 we developed a novel method for calculating response curves for periodically driven oscillators. We derived an expression for the steady state energy of a sinusoidally driven damped oscillator in terms of the action, the first Fourier coefficient and its derivative with respect to energy.

In chapter 5 we showed excellent agreement between numerical simulations of a sinusoidally driven highly nonlinear Duffing oscillator with response curves calculated by the new methods of chapter 4.

In chapter 6 we derived an expression for the frequency of two-way coupled oscillators when they are phased-locked; we call this the locking frequency.

In chapter 7 we showed excellent agreement between locking frequencies calculated by numerical simulations of two coupled van der Pol oscillators with highly nonlinear Duffing forces and by the corresponding expressions from the theory of chapter 6.

In chapters 5 and 7 we calculated explicit analytic expressions for the constants, a_i, in the standard equation for two separate oscillator systems, a sinusoidally driven highly nonlinear Duffing oscillator (force $\sim -x^3$), and two coupled van der Pol oscillators with highly nonlinear Duffing forces. For both systems, numerical simulations of the Φ–Ω trajectories were calculated from the original ODEs and the corresponding standard equation. The standard equation's trajectories appeared to be a smoothed shadow of the original ODE's trajectories, even in parameter regions near topographical transitions.

8.2 Future Work

In this paper we have analytically and numerically studied two types of coupled librating oscillators. However, the analytical methods used in this paper (i.e., the transformation functions and averaging method) can be used to study coupled oscillators with other types of coupling forces and coupled rotating oscillators. This can be applied to find conditions for phase-locked rotational states in weakly damped coupled Josephson junctions and driven charge density waves. In addition, the action-angle transformation functions could be applied to more than two coupled oscillators, such as chains of coupled Josephson junctions [25, 9, 26, 27].

Most physical systems are not completely isolated from external influence. External influences can sometimes be modeled collectively by dissipative forces in a low-dimensional model of the system. If this is the case then all the applications that were modeled by coupled conservative oscillators can now be studied with a more realistic model that includes dissipative terms at an early stage in the development of the model by using the methods developed in this paper.

For example, in studying resonances in celestial mechanics, Ghil and Wolansky [28] introduce dissipative "forces" to an asteroid circling the sun with a perturbation from the gravitational pull of Jupiter. In this case the dissipative forces are due to collisions of the celestial body with a small cloud of particles. The dissipative "forces" are introduced to the system after changing to action-angle variables. This is because it is not possible to include dissipative terms when applying the Hamiltonian transformation to get to action-angle variables. Because of this, it is unclear how the terms associated with the dissipation are related to the more fundamental physical forces from the collisions. With the methods developed here it is possible to include dissipative terms when transforming the system to action-angle variables. So, one can develop a more fundamental physical model of the dissipative forces and then apply the transformation to action-angle variables and see how the dissipative terms in the resonant dynamics depend on fundamental physical parameters. Of course, in order to apply our transformations, we need to expand our transformations to apply to higher dimensional systems.

In addition to applications in celestial mechanics, other possible applications are non-linear resonances in: electrical circuits, mechanical systems [6], plasma oscillations [29], and particle beam dynamics [30].

Appendix A

Generalized Action-Angle Variables

In this appendix we develop action-angle variables for a single one-dimensional oscillating system. In the preceding chapters we have added damping perturbations to the single oscillator. In order to do so, we had to define action-angle variables with more generality than the usual Hamiltonian formulation of action-angle variables. To accomplish this the action-angle variables were defined by transformation functions as opposed to generating functions of a Hamiltonian formulation.

We start by reviewing some of the properties of action-angle variables as defined for a Hamiltonian system, then we use these properties to present the transformation functions that define our generalized action-angle variables, and finally we derive the equations of motion for these generalized action-angle variables when a general perturbation is added to the single oscillator.

A.1 Review of Action-Angle Variables

We can use Hamiltonian methods to solve the unperturbed single oscillator system

$$\dot{x}_0 = \frac{p_0}{m}, \tag{A.1}$$

$$\dot{p}_0 = F(x_0), \tag{A.2}$$

$$F(x_0) \equiv -\frac{dU(x_0)}{dx_0}, \tag{A.3}$$

where x_0 and p_0 are a pair of canonical variables, U is the potential of the oscillator, and m is a constant. Eqs. (A.1) and (A.2) can be derived from the Hamiltonian

$$H_0(x_0, p_0) = U(x_0) + \frac{p_0^2}{2m}. \tag{A.4}$$

We restrict the solutions of Eqs. (A.1) and (A.2) such that the motion of p_0 is periodic and we have either libration or rotation type motion [31].

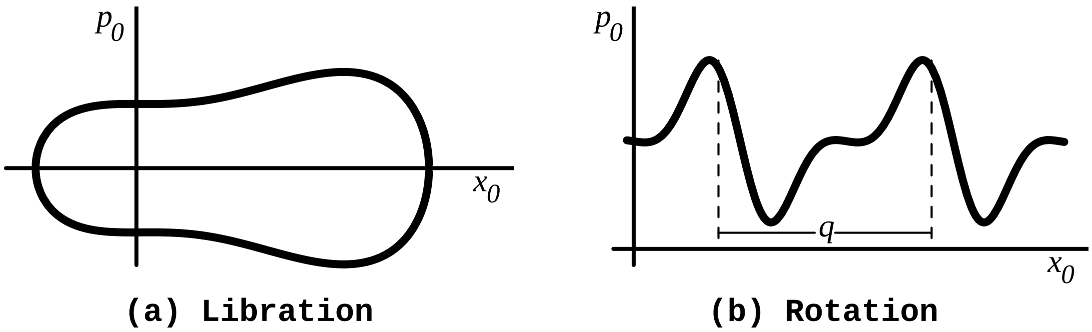

Figure A.1: The phase-space portrait of the two types of periodic motion of one-dimensional conservative systems.

In libration, both x_0 and p_0 are periodic in time; a phase-plot of p_0 vs. x_0 is a closed curve as in Fig. A.1 (a). The most common example of librator is a simple harmonic oscillator.

To have rotation, the potential, $U(x_0)$, must be periodic in x_0. In rotation, p_0 is periodic in time and x_0 is increasing without bound; in a phase-plot of p_0 vs. x_0, p_0 is a periodic function of x_0 as in Fig. A.1 (b). A cycle of oscillation is when x_0 increases by q, the least amount that $U(x_0)$ is periodic in. The most common physical example of a rotating oscillator is a pendulum that is rotating in full circles in a vertical plane, where the angular position and the angular momentum of the pendulum are the two canonical variables x_0 and p_0 respectively.

We introduce the action-angle variables J_0 and ϕ_0, of the unperturbed system, by

$$J_0 = \frac{1}{2\pi} \oint p_0 dx_0, \tag{A.5}$$

where the integration is carried over a complete cycle of the oscillation for libration or rotation and ϕ_0 is the coordinate conjugate to J_0. The action, J_0, can be interpreted geometrically as the area enclosed by the phase-plots of the oscillator in Fig. A.1.

The equations of motion for ϕ_0 and J_0 are

$$\dot{\phi}_0 = \omega_0(J_0), \tag{A.6}$$

$$\dot{J}_0 = 0, \tag{A.7}$$

$$\omega_0(J_0) = \frac{\partial K_0(J_0)}{\partial J_0}, \tag{A.8}$$

where $K_0(J_0)$ is the Hamiltonian of the unperturbed system when it is transformed to action-angle variables and $\omega_0(J_0)$ is the angular frequency of the unperturbed system.

A.2 Action-Angle Transformation Functions

We define transformation functions P_0 and X_0, such that

$$x_0 = X_0(J_0, \phi_0), \tag{A.9}$$

$$p_0 = P_0(J_0, \phi_0). \tag{A.10}$$

From Eqs. (A.1), (A.2), (A.9), and (A.10)

$$\frac{\partial X_0}{\partial J_0}\dot{J}_0 + \frac{\partial X_0}{\partial \phi_0}\dot{\phi}_0 = \frac{P_0}{m}, \tag{A.11}$$

$$\frac{\partial P_0}{\partial J_0}\dot{J}_0 + \frac{\partial P_0}{\partial \phi_0}\dot{\phi}_0 = F(X_0). \tag{A.12}$$

From Eqs. (A.6), (A.7), (A.11), and (A.12)

$$\omega_0(J_0)\frac{\partial X_0}{\partial \phi_0} = \frac{P_0}{m}, \tag{A.13}$$

$$\omega_0(J_0)\frac{\partial P_0}{\partial \phi_0} = F(X_0). \tag{A.14}$$

Given these transformation functions, the transformed Hamiltonian of the unperturbed system, $K_0(J_0)$, is

$$K_0(J_0) = U(X_0) + \frac{P_0^2}{2m}. \tag{A.15}$$

Eqs. (A.8) and (A.13)–(A.15), along with the equation

$$J_0 = \frac{1}{2\pi} \oint P_0 dX_0, \tag{A.16}$$

where the integration is over one cycle of X_0 and P_0 as ϕ changes from 0 to 2π, can be used to define the transformation functions $X_0(J_0, \phi_0)$ and $P_0(J_0, \phi_0)$ to within an arbitrary constant.

Now we study the perturbed single oscillator system,

$$\dot{x} = \frac{p}{m}, \tag{A.17}$$

$$\dot{p} = F(x) + \Lambda(x, p, \zeta, t), \tag{A.18}$$

$$F(x) \equiv -\frac{dU(x)}{dx}, \tag{A.19}$$

where x and p are independent dynamical variables, m is a constant, Λ is the perturbation, ζ represents other time-dependent variables that are distinct from p and x, t is time, and U is functionally the same as the function U in Eq. (A.3). ζ can contain variables from other systems.

We do not restrict Λ such that it can be derived from a potential. Because of this, we cannot use Hamiltonian methods to solve Eqs. (A.17) and (A.18). In what follows we will refer to Eqs. (A.17) and (A.18) with $\Lambda \equiv 0$ as the unperturbed oscillator.

We transform x and p, in Eqs. (A.17) and (A.18), to the action-angle variables, J and ϕ, by using

$$x = X(J, \phi), \tag{A.20}$$

$$p = P(J, \phi), \tag{A.21}$$

where $X(J, \phi)$ and $P(J, \phi)$ satisfy

$$\omega(J)\frac{\partial X}{\partial \phi} = \frac{P}{m}, \tag{A.22}$$

$$\omega(J)\frac{\partial P}{\partial \phi} = F(X), \tag{A.23}$$

$$J = \frac{1}{2\pi} \oint P dX, \tag{A.24}$$

$$K(J) = U(X) + \frac{P^2}{2m}, \tag{A.25}$$

$$\omega(J) = \frac{\partial K(J)}{\partial J}, \tag{A.26}$$

where the integration is carried over a complete cycle of $X(J, \phi)$ and $P(J, \phi)$ as they change when ϕ goes from 0 to 2π with J held constant.

To within a constant, the transformation functions X and P are functionally the same as X_0 and P_0 respectively. So that the transformation functions $X(J, \phi)$ and $P(J, \phi)$ are unique, we impose the following boundary conditions that depend on whether the motion of the unperturbed oscillator is libration or rotation. For the case when the unperturbed oscillator librates (libration case) we impose,

$$P(J, 0) = 0, \tag{A.27}$$

$$F(X(J, 0)) < 0. \tag{A.28}$$

For the case when the unperturbed oscillator rotates (rotation case) we impose,

$$X(J, 0) = 0, \tag{A.29}$$

$$P(J, 0) > 0. \tag{A.30}$$

The general solution to Eqs. (A.22)–(A.26) can be written as:
for the libration case with the conditions Eqs. (A.27) and (A.28),

$$X(J, \phi) = \sum_{l=0}^{\infty} C_l(J) \cos(l\phi), \tag{A.31}$$

$$P(J, \phi) = -m\omega(J) \sum_{l=1}^{\infty} lC_l(J) \sin(l\phi), \tag{A.32}$$

for the rotation case with the conditions Eqs. (A.29) and (A.30),

$$X(J, \phi) = \frac{\phi}{2\pi} q + \sum_{l=1}^{\infty} C_l(J) \sin(l\phi), \tag{A.33}$$

$$P(J, \phi) = m\frac{\omega(J)}{2\pi} q + m\omega(J) \sum_{l=1}^{\infty} lC_l(J) \cos(l\phi), \tag{A.34}$$

where $C_l(J)$ is a Fourier coefficient that is dependent on J, and q is the smallest constant to satisfy $U(x+q) = U(x)$. The Fourier coefficients, $C_l(J)$, are the same action-dependent

Fourier coefficients as in the solution of the unperturbed oscillator. $x = X(J, \omega(J)t + \phi)$ and $p = P(J, \omega(J)t + \phi)$ is the solution of the unperturbed oscillator, where J and ϕ are the initial action and angle respectively.

A.3 Dynamics of Generalized Action-Angle Variables

We now find the equations of motion for the perturbed system Eqs. (A.17) and (A.18) in terms of action-angle variables, J and ϕ, that are defined by Eqs. (A.20)–(A.26). From Eqs. (A.17), (A.18), (A.20), and (A.21)

$$\frac{\partial X}{\partial \phi}\dot{\phi} + \frac{\partial X}{\partial J}\dot{J} = \frac{P}{m}, \tag{A.35}$$

$$\frac{\partial P}{\partial \phi}\dot{\phi} + \frac{\partial P}{\partial J}\dot{J} = F(X) + \Lambda(X, P, \zeta, t). \tag{A.36}$$

Solving the above for $\dot{J}$ and $\dot{\phi}$ gives

$$\dot{\phi} = \frac{\frac{P}{m}\frac{\partial P}{\partial J} - [F(X) + \Lambda(X, P, \zeta, t)]\frac{\partial X}{\partial J}}{\frac{\partial X}{\partial \phi}\frac{\partial P}{\partial J} - \frac{\partial X}{\partial J}\frac{\partial P}{\partial \phi}}, \tag{A.37}$$

$$\dot{J} = \frac{[F(X) + \Lambda(X, J, \zeta, t)]\frac{\partial X}{\partial \phi} - \frac{P}{m}\frac{\partial P}{\partial \phi}}{\frac{\partial X}{\partial \phi}\frac{\partial P}{\partial J} - \frac{\partial X}{\partial J}\frac{\partial P}{\partial \phi}}. \tag{A.38}$$

Taking the derivative of Eq. (A.25) with respect to J, substituting $F(X)$ for $-\frac{dU(X)}{dX}$, followed by using Eqs. (A.22), (A.23), and (A.26) for substitutions for $F(X)$, $\frac{P}{m}$, and $\frac{\partial K(J)}{\partial J}$ respectively and rearranging gives

$$\frac{\partial X}{\partial \phi}\frac{\partial P}{\partial J} - \frac{\partial X}{\partial J}\frac{\partial P}{\partial \phi} = 1. \tag{A.39}$$

Eq. (A.39) shows that the Jacobian of this transformation is 1, which implies that this transformation is canonical according to Percival [32]. With Eqs. (A.22), (A.23), and (A.37)–(A.39), the equation of motion of the perturbed system in the generalized action-angle variables, J and ϕ, becomes

$$\dot{\phi} = \omega(J) - \frac{\partial X(J, \phi)}{\partial J}\Lambda, \tag{A.40}$$

$$\dot{J} = \frac{\partial X(J, \phi)}{\partial \phi}\Lambda, \tag{A.41}$$

where $\Lambda = \Lambda(X(J,\phi), P(J,\phi), \zeta, t)$. It should be noted that there are no approximations in deriving Eqs. (A.40) and (A.41).

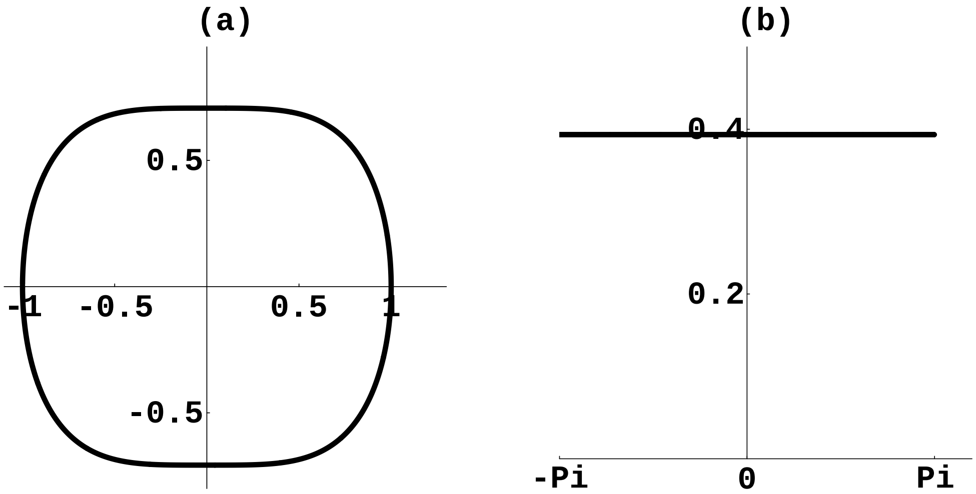

Figure A.2: Phase plots for a librating oscillator without perturbations: (a) p vs. x and (b) J vs. ϕ; from a numerical integration of Eqs. (A.17)–(A.19) with $U(x) = \frac{1}{4}x^4$, $m = 1$, and $\Lambda = 0$.

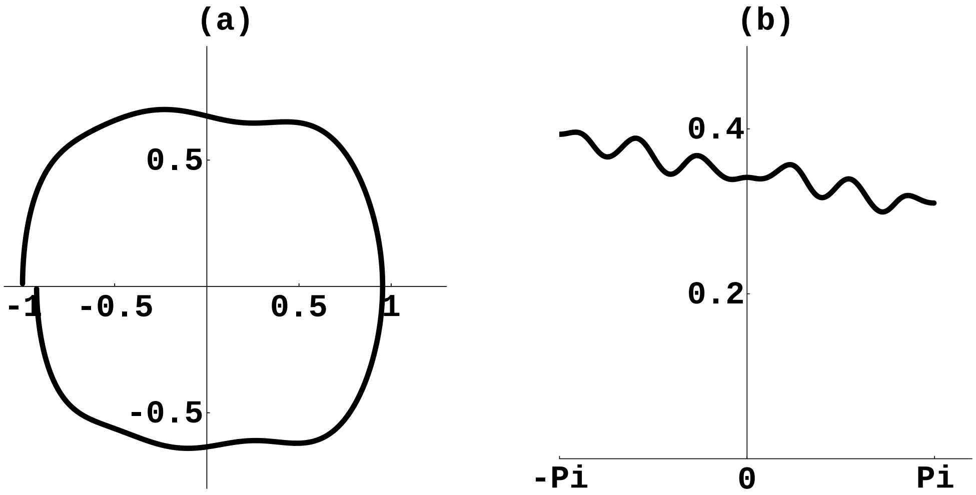

Figure A.3: Phase plots for a librating oscillator with perturbations: (a) p vs. x and (b) J vs. ϕ; from a numerical integration of Eqs. (A.17)–(A.19) with $U(x) = \frac{1}{4}x^4$, $m = 1$, and $\Lambda = -\gamma p + \mathcal{A}\cos(\varpi t)$, where $\gamma = 0.03$, $\mathcal{A} = 0.1$, and $\varpi = 5$.

Appendix B

The Averaging Approximation

In this paper we extensively used the method of averaging. In many cases it can be shown that averaging is the first order approximation to an asymptotic series [12, 33]. For this reason we consider our calculations a first-order perturbation theory.

In this appendix we will analyze the averaging methods that we have used. We will show how well the ϕ-averaged equations of chapters 2, 3, 4, and 6 represent a sliding time-average of the exact equations of motion.

B.1 What Do These Averaged ODEs Represent?

We consider the system

$$\dot{z} = \epsilon f(\phi, z), \quad z, f \in \Re^3, \quad f(\phi + 2\pi, z) = f(\phi, z), \tag{B.1}$$

$$\dot{\phi} = g(z) + \epsilon h(\phi, z) > 0, \quad \phi, g, h \in \Re^1, \tag{B.2}$$

where ϵ is a small constant and we assume that all other quantities are of size of order 1. We will refer to this system as the exact system.

The vector variable z and the corresponding variables that were used in the chapters are:

$$z = \{\Phi, \Omega, I\}\,, \ \text{ in chapters 2 and 6 in Eqs. (2.9)–(2.12);}$$

$$z = \{\Phi, K_2, E_T\}\,, \quad \text{in chapter 3 in Eqs. (3.10)–(3.13);}$$
$$z = \{J_1, K_2, \Phi\}\,, \quad \text{in chapter 4 in Eqs. (4.8)–(4.11).}$$

We define a sliding time-averaged function $\overline{\xi(t)}$ as

$$\overline{\xi(t)} = \frac{1}{T}\int_{t'=t-\frac{T}{2}}^{t+\frac{T}{2}} \xi(t')dt', \tag{B.3}$$
$$T \equiv \frac{2\pi}{g(z(t))}. \tag{B.4}$$

We note that, since T is a function of t, it is not in general true that $\overline{\dot{\xi}(t)} = \dot{\overline{\xi(t)}}$.

From Eqs. (B.1) and (B.3)

$$\begin{aligned}\overline{\dot{z}(t)} &= \frac{\epsilon}{T}\int_{t'=t-\frac{T}{2}}^{t+\frac{T}{2}} f(\phi(t'), z(t'))dt' = \frac{z(t+\frac{T}{2}) - z(t-\frac{T}{2})}{T} \\ &= \frac{\epsilon}{T}\int_{t'=t-\frac{T}{2}}^{t+\frac{T}{2}} \left[f(\phi(t'), z(t)) + \sum_{i=1}^{3}\frac{\partial f(\phi(t'), z(t))}{\partial z_i(t)}\epsilon f_i(\phi(t), z(t))\,(t'-t)\right] dt' \\ &= \frac{\epsilon}{T}\int_{t'=t-\frac{T}{2}}^{t+\frac{T}{2}} f(\phi(t'), z(t))dt' + \mathcal{O}(\epsilon^2),\end{aligned} \tag{B.5}$$

where z_i is the i-th component of z, f_i is the i-th component of f, and $\mathcal{O}(\epsilon^2)$ represents terms of size of order ϵ^2.

Because ϕ is an increasing function of t, we can write t as a function of ϕ and vice versa. So, we proceed to change integration variables in Eq. (B.5) from t' to ϕ'. From Eq. (B.2)

$$\begin{aligned}d\phi' &= \left(g(z(t')) + \epsilon h(\phi'(t'), z(t'))\right) dt' \\ &= g(z(t))dt' + \mathcal{O}(\epsilon) \\ &= \frac{2\pi}{T(t)}dt' + \mathcal{O}(\epsilon),\end{aligned} \tag{B.6}$$

where we have used the fact that $\dot{z} = \mathcal{O}(\epsilon)$ from Eq. (B.1) and that $t' - t = \mathcal{O}(1)$ for all values of the t' in the interval of integration of Eq. (B.5).

The limits of integration are changed to

$$\phi' = \phi(t \pm \frac{T(t)}{2})$$

$$
\begin{aligned}
&= \phi(t) + \int_{t''=t}^{t\pm\frac{T(t)}{2}} g(z(t''))dt'' + \mathcal{O}(\epsilon) \qquad\qquad \text{(B.7)}\\
&= \phi(t) \pm g(z(t))\frac{T(t)}{2} + \sum_{i=1}^{3}\frac{\partial g(z(t))}{\partial z_i(t)}\epsilon f_i(\phi(t),z(t))\int_{t''=t}^{t\pm\frac{T(t)}{2}}(t''-t)dt'' + \mathcal{O}(\epsilon)\\
&= \phi \pm \pi + \mathcal{O}(\epsilon).
\end{aligned}
$$

From this and Eq. (B.5)

$$
\begin{aligned}
\overline{\dot{z}(t)} &= \frac{\epsilon}{2\pi}\int_{\phi'=\phi-\pi+\mathcal{O}(\epsilon)}^{\phi+\pi+\mathcal{O}(\epsilon)} f(\phi', z(t'(\phi')))d\phi' + \mathcal{O}(\epsilon^2)\\
&= \frac{\epsilon}{2\pi}\int_{\phi'=\phi-\pi}^{\phi+\pi} f(\phi', z(t))d\phi' + \frac{\epsilon}{2\pi}\int_{\phi'=\phi-\pi}^{\phi+\pi}\sum_{i=1}^{3}\frac{\partial f(\phi', z(t))}{\partial z_i(t)}\epsilon f_i(\phi, z(t))(t'(\phi')-t)d\phi' + \mathcal{O}(\epsilon^2)\\
&= \frac{\epsilon}{2\pi}\int_{\phi'=\phi-\pi}^{\phi+\pi} f(\phi', z(t))d\phi' + \mathcal{O}(\epsilon^2), \qquad\qquad \text{(B.8)}
\end{aligned}
$$

where $t'(\phi')$ is the inverse of the function $\phi(t)$ with $\phi = \phi'$ and $t = t'$, and $z(t)$ is independent of ϕ'.

Since f is a periodic function of ϕ, we get

$$
\overline{\dot{z}(t)} = \frac{1}{2\pi}\int_{\phi'=0}^{2\pi}\epsilon f(\phi', z(t))d\phi' + \mathcal{O}(\epsilon^2). \qquad\qquad \text{(B.9)}
$$

Thus, to order ϵ^2 the ϕ-averaged equations of motion are a floating time-averaged value of the exact equations of motion.

References

[1] A. J. Lichtenberg, and M. A. Lieberman. *Regular and Chaotic Dynamics*. Springer-Verlag, New York, N.Y., 2nd edition, 1992.

[2] T. Eisenhammer, A. Hübler, T. Geisel, and E. Lücher. Scaling behavior of the maximum energy exchange between coupled anharmonic oscillators. *Physical Review A*, 41(6):3332–42, March 1990.

[3] A. H. Nayfeh, and D. T. Mook. *Nonlinear Oscillations*. Wiley, New York, N.Y., 1979.

[4] Y. Kuramoto. *Chemical Oscillations, Waves, and Turbulence*. Springer-Verlag, New York, N.Y., 1984.

[5] T. Bohr, P. Bak, and M. H. Jensen. Transition to chaos by interaction of resonances in dissipative systems. ii. josephson junctions, charge-density waves, and standard maps. *Physical Review A*, 30(4):1970–81, October 1984.

[6] E. Atlee Jackson. *Perspectives of Nonlinear Dynamics, Volume 1*, chapter 5. Cambridge University Press, New York, N.Y., 1991.

[7] J. Guckenheimer, and P. Holmes. *Nonlinear Oscillations, Dynamical Systems, and Bifurcations of Vector Fields*. Springer-Verlag, New York, N.Y., 1983.

[8] James Murdock. Qualitative theory of nonlinear resonances by averaging and dynamical systems methods. In U. Kirchgraber, and H. O. Walther, editor, *Dynamics Reported*, volume 1. Wiley and B. G. Teubner, New York, N.Y., 1988.

[9] Steve Nichols, and Kurt Wiesenfeld. Ubiquitous neutral stability of splay-phase states. *Physical Review A*, 45(12):8430–5, June 1992.

[10] Jeremy Levy, and Mark S. Sherwin. Time-domain study of low-dimensional chaos in the switching charge-density-wave conductors in $NbSe_3$. *Physical Review Letters*, 70(17):2597–600, April 1993.

[11] B. R. Noack, F. Ohle, and H. Eckelmann. Construction and analysis of differential equations from experimental time series of oscillatory systems. *Physica D*, 56:389–405, 1992.

[12] N. N. Bogoliubov, and Y. A. Mitropolsky. *Asymptotic Methods in the Theory of Non-Linear Oscillations*. Gordon & Breach, New York, N.Y., 1961.

[13] Chihiro Hayashi. *Nonlinear Oscillations in Physical Systems*. Princeton University Press, Princeton, New Jersey, 1964.

[14] A. H. Nayfeh, and D. T. Mook. *Nonlinear Oscillations*, pages 163–74. Wiley, New York, N.Y., 1979.

[15] Boris V. Chirikov. A universal instability of many-dimensional oscillator systems. *Physics Reports*, 52(4):263–379, 1979.

[16] V. I. Arnold. Small denominators and problems of stability of notion in classical and celestial mechanics. *Russian Mathematical Surveys*, 18(6):85–189, 1963.

[17] Lance E. Arsenault, and Alfred W. Hübler. Dynamics of damped coupled oscillators near resonance. *Physical Review E*, 51(4):3561–71, April 1995.

[18] J. K. Hale. *Ordinary Differential Equations*. Wiley, New York, N.Y., 1969.

[19] J. A. Sanders, and F. Verhulst. *Averaging Methods in Nonlinear Dynamical Systems*. Springer-Verlag, New York, N.Y., 1985.

[20] Gregor Dellemann, Lance E. Arsenault, Dan Bensen, and Alfred W. Hübler. Nonlinear resonance spectroscopy with aperiodic forcing functions of constant amplitude. submitted to: *Physical Review Letters*.

[21] A. H. Nayfeh, and D. T. Mook. *Nonlinear Oscillations*, pages 175–9. Wiley, New York, N.Y., 1979.

[22] A. H. Nayfeh, and D. T. Mook. *Nonlinear Oscillations*, page 165. Wiley, New York, N.Y., 1979. Eqs. (4.39) and (4.40) are the same as (4.1.16) in this reference with $A_{2,f} \to a$, $\gamma \to 2\mu$, $\Phi \to \gamma$, $\omega_2 \to \omega_0$, $A_1 \to k$, and $\omega_1 - \omega_2 \to \sigma$.

[23] I. S. Gradshteyn, and I. M. Ryzhik. *Table of Integrals, Series, and Products*, pages 910–7. Academic Press, San Diego, California, 1980.

[24] Lance E. Arsenault, and Alfred W. Hübler. Dynamics of damped coupled oscillators near resonance. *Physical Review E*, 51(4):3561–71, April 1995. See pages 3566–7 for details of changing the coupled Van der Pol oscillators to dimensionless equations.

[25] P. Hadley, M. R. Beasley, and K. Wiesenfeld. Phase locking of josephson-junction series arrays. *Physical Review B*, 38(13):8712–9, November 1988.

[26] K. Y. Tsang, S. H. Stogatz, and K. Wiesenfeld. Phase locking of josephson-junction series arrays. *Physical Review Letters*, 66(8):1094–7, February 1991.

[27] K. Y. Tsang, and I. B. Schwartz. Interhyperhedral diffusion in josephson-junction arrays. *Physical Review Letters*, 68(15):2265–8, April 1992.

[28] M. Ghil, and G. Wolansky. Non-hamiltonian perturbations of integrable systems and resonance trapping. *SIAM Journal of Applied Mathematics*, 52(4):1148–71, August 1992.

[29] M. Deutsch, B. Meerson, and J. E. Golub. Strong plasma wave excitation by a *chirped* laser beat wave. *Physics of Fluids B*, 3(7):1773–80, July 1991.

[30] S. Y. Lee. Single-particle dynamics at synchro-betatron coupling resonances. *Physical Review E*, 49(6):5706–16, June 1994.

[31] Herbert Goldstein. *Classical Mechanics*, chapter 10-5. Addison-Wesley, Reading, Massachusetts, 2nd edition, 1980.

[32] Ian Percival, and Derek Richards. *Introduction to Dynamics*, page 85. Cambridge University Press, New York, N.Y., 1982.

[33] Martin Kruskal. Asymptotic theory of hamiltonian and other systems with all solutions nearly periodic. *Journal of Mathematical Physics*, 3(4):806–28, July–August 1962.

Vita

Lance Eric Arsenault
Born: April 28, 1960, Taunton, Massachusetts, USA.

Education

Ph.D., Physics, University of Illinois at Urbana-Champaign (UIUC), 1996
M.S., Physics, University of Illinois at Urbana-Champaign, 1989
B.S., Physics, University of Massachusetts (UMass) at Dartmouth, 1986

Honors

Excellence in Teaching Award, UIUC Department of Physics, Spring Semester 1994
Member, Sigma Pi Sigma, The National Physics Honor Society

Publications

Gregor Dellemann, Lance E. Arsenault, Dan Bensen, and Alfred W. Hübler. Nonlinear resonance spectroscopy with aperiodic forcing functions of constant amplitude, submitted to: *Physical Review Letters*

Lance E. Arsenault, and Alfred W. Hübler. Dynamics of damped coupled oscillators near resonance. *Physical Review E*, 51(4):3561–71, April 1995.

K. Kishino, M. S. Ünlü, J. I. Chyi, J. Reed, L. Arsenault, and H. Mockoç. Resonant cavity-enhanced (RCE) photodetectors. *IEEE Journal of Quantum Electronics*, 27(8):2025–34, August 1991.

Teaching and Professional Experience

3/91 - 1/96 **Teaching/Research Assistant**, UIUC Department of Physics. Conducted research in conjunction with Alfred W. Hübler. Programmer/Developer on the CyberProf Project.

9/90 - 3/91 **Teaching Assistant**, UIUC Department of Physics. Taught introductory undergraduate physics classes.

1/89 - 9/90 **Research Assistant**, UIUC Department of Physics. Conducted research in conjunction with Hadis Mockoç on molecular beam epitaxial growth of III-V semiconductors.

9/87 - 1/89 **Teaching Assistant**, UIUC Department of Physics. Taught introductory undergraduate physics classes.

9/86 - 6/87 **Teaching Assistant**, UMass at Dartmouth Department of Physics. As graduate student, worked as an undergraduate laboratory instructor.

9/81 - 9/86 **Carpenter and a Short-order Cook**. While an undergraduate.

7/78 - 7/81 **U.S. Marine Corps**. Performed maintenance on earth-moving equipment as Heavy Equipment Mechanic (MOS 1341).